ISSN1346－7832

独立行政法人港湾空港技術研究所

港湾空港技術研究所報告

REPORT OF THE PORT AND AIRPORT RESEARCH INSTITUTE

VOL.41 NO.2 June 2002

NAGASE, YOKOSUKA, JAPAN

INDEPENDENT ADMINISTRATIVE INSTITUTION,
PORT AND AIRPORT RESEARCH INSTITUTE

港湾空港技術研究所報告（REPORT OF PARI）
第 41 巻　第 2 号（Vol.41, No.2），2002年6月（June 2002）

目　次（CONTENTS）

REPORT OF THE PORT AND
AIRPORT RESEARCH INSTITUTE
VOL.41, NO.2 (June,2002)

Evaluation of structure and mechanical properties of Pleistocene clay in Osaka Bay

Takashi TSUCHIDA*
Yoichi WATABE**
Min-Soo KANG***

Synopsis

In recent years, as the scale of structures has been enlarged and the construction works have been carried out in deeper sea areas, the loads due to constructions has become close or larger than the consolidation yield stress, p_c, of the Pleistocene clay layer beneath the Holocene layers. In this report, the compression and shear characteristics of aged Pleistocene clay in Osaka Bay, were reviewed with related to the case study on Kansai International Airport project.

1) The concept of standard compression curve (SCC) of marineclays was proposed. The standard compression curve consists of ultimate standard compression curve, USC, and the standard compression curves from an initial void ratio, SCC(e_0). Both curves are determined mainly by the liquid limit of clay and the void ratio at the beginning of consolidation. Using the specific volume index, I_{sv}, defined as ln $(1+e)$ / ln $(1+e_L)$, USC and SCC(e_0) were given as a unique I_{sv} – log p relationship.
2) By comparing in-situ specific volume of clay with value on of SCC, the degree of structure of marine deposits can be evaluated. It is shown that Osaka Bay Pleistocene clay seems to have well-developed structure due to aging, because the in-situ values of I_{sv} are much larger than those of SCC-marine.
3) The consolidation characteristics of Osaka Pleistocene clay was examined with the purpose of investigating soil structural effect. At the pressure increment spanning the consolidation yield stress, effective stress increasing with elapsed time showed sudden decreasing tendency. The cause of this unique behavior seems to be attributed to the fact that radical increase of compressibility by the yielding of soil structure would surpasse the excess pore pressure dissipation. This behavior is particularly relevant to clays with a well-developed structure such as Osaka Pleistocene clay.
4) The undrained shear strengths and deformation characteristics of Pleistocene clay were studied by the recompression method with triaxial tests. The Pleistocene clay at large depths is brittle and shifts very rapidly from elastic deformation to plastic failure. Although the safety factor of slip circle which passes through the Pleistocene clay layer was larger than 1.20, the margin of the safety were not so much. The accurate estimation of the shear strength of Pleistocene clays and the field observations and construction control will be necessary to complete the projects safely.

Key Words: compression, consolidation, Pleistocene clay, shear strength, stability analysis

* Head of Soil Mechanics and Geo-environment Division
** Senior Researcher of Soil Mechanics and Geo-environment Division
*** Researcher of Soil Mechanics and Geo-environment Division
Port and Airport Research Institute, 3-1-1 Nagase, Yokosuka, 239-0826, Japan
Phone : +81-468-445053 Fax : +81-468-444577 e-mail:tsuchida@pari.go.jp

港湾空港技術研究所報告
第41巻第2号(2002年6月)

大阪湾洪積粘土の構造の評価と力学特性

土田　孝*
渡部　要一**
姜　敏秀***

要　旨

近年、港湾や空港事業が沖合に進出した結果、沖積粘土層の下部にある洪積粘土地盤の圧密沈下の予測やせん断強さの評価が設計上大きな問題になっている。本研究は、一連の室内土質試験結果に基づいて大阪湾洪積粘土の堆積構造の評価とその力学特性を検討しており、以下のような結論が得られた。

1) 自然に堆積した海底地盤を対象とした基準圧縮曲線の概念を誘導した。わが国の多くの沖積粘土地盤では原位置の間隙比に関して顕著な構造の影響はみられなかった。しかし、関西国際空港が立地する大阪湾泉南沖海底の洪積粘土地盤では、堆積ひずみに換算して5～15%に相当する構造が形成されており、このことが沖積粘土地盤よりも大きい圧縮性を示す原因であると考えられる。
2) 分割圧密試験の結果，過圧密領域から正規圧密領域に移行する過程にお間隙水圧が再び上昇するという非常にユニークな現象がみられた．これは、圧密中に構造が破壊するためであると考えられる。
3) 深度の大阪湾洪積粘土は，弾性的な変形から急激に破壊へ移行する脆性的な力学特性を示した。特に、伸張においても3～4%のひずみで明確な軸差応力のピークが現れた．
4) 関西国際空港の代表的な緩傾斜護岸を用いた想定断面を対象として安定解析を行った結果、伸張強度の定義の仕方により，すべり円弧の通過点は沖積層内に収まるか，洪積層にまで達するかが大きく異なった．いずれの場合にも，安全率は 1 以上であるが、その余裕は大きくないので設計施工においてはすべりに対する安定に十分留意する必要がある．

キーワード：粘土、せん断，圧縮，圧密、三軸試験、洪積層、年代効果、安定解析

* 地盤・構造部土質研究室長
** 地盤・構造部主任研究官
*** 地盤・構造部土質研究室研究官

〒239-0826　横須賀市長瀬3-1-1　独立行政法人港湾空港技術研究所
電話：0468-44-5053　Fax：0468-44-4577　e-mail:tsuchida@pari.go.jp

CONTENTS

1. Introduction

In the research of soil mechanics, remolded and reconstituted clays have been used in laboratory test to avoid scatter of experimental results. However, it was clarified that mechanical properties of remolded clays are quite different from those of natural clays, because natural clay has a structure due to secondary compression and/or cementation effects during sedimentation. (Tavenas and Leroueil, 1977; Jamiolkowski et al., 1985). Although these differences are observed in Holocene clays, they have raised important engineering problems in the construction projects on Pleistocene clays layers.

In coastal regions of Japan, Pleistocene clay layer is often located beneath a Pleistocene gravel layer, which lies under a 5 to 30 m thick Holocene clay layer. In most construction projects before 1970, the Pleistocene gravel layer had been considered as a stable layer that could support the superstructures, and the engineers seldom consider the behavior of Pleistocene clay layers beneath the gravel layer. In recent years, however, as the scale of structures has been enlarged and the construction works have been carried out in deeper sea areas, the loads due to constructions has become close to or larger than the consolidation yield stress, p_c, of the Pleistocene clay layer at large depth. Thus, the evaluation on engineering properties of the Pleistocene clay layer is one of the most important issues for design and construction in the coastal areas.

As a typical example, **Figure 1** shows time-settlement curves obtained from 4 corners of a ventilation tower for undersea tunnel constructed at a reclaimed land in Osaka Port (Nakashima et al., 1995). The ventilation tower was constructed at the depth of 33.5m trenched down to the top of Pleistocene gravel layer. However, as shown in **Figure 2,** the soil profiles in the site, below the gravel layer, there exist three Pleistocene clay layers whose over-consolidation ratios were 1.8 – 2.3 before construction. As the reclamation continued after the installation of the ventilation tower, the overburden stress on Pleistocene clay layers was increased consequently decreasing the over-consolidation ratios. **Figure 3** is OCR profiles of Pleistocene clay layers after the completion of reclamation, showing that all the layers are still in the over-consolidated regions. Although the overburden stress did not exceed the consolidation yield stress, the settlements of 50-130cm have taken place continuously for 2500 days. According to Nakashima et al., the predicted settlements with coefficient of volume compressibility, m_v and coefficient of consolidation, c_v, obtained by conventional step loading consolidation tests underestimated the observed settlements, and to explain the observed settlement, it was necessary to use larger compressibility m_v and

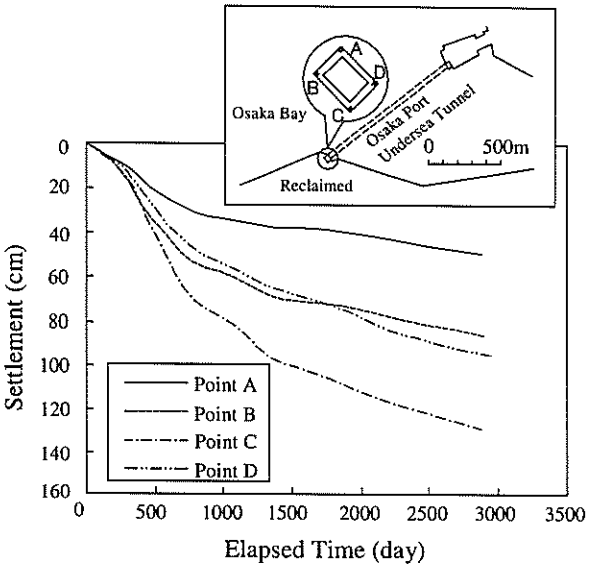

Figure 1 Settlement of ventilation tower of undersea tunnel in Osaka Port

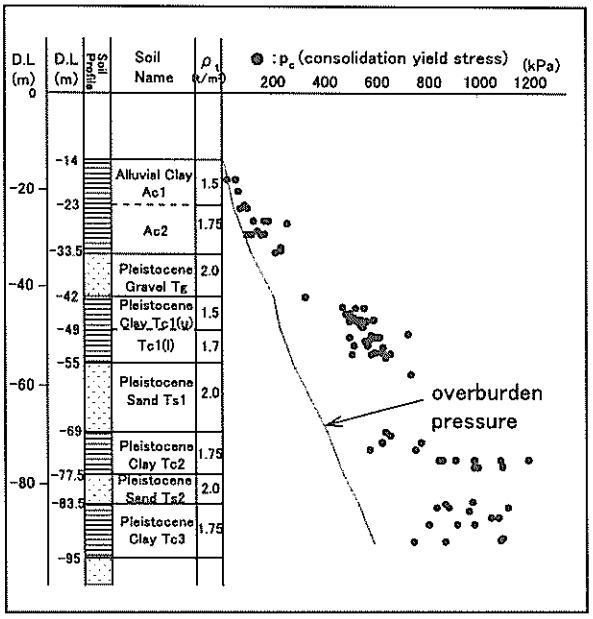

Figure 2 Soil profiles at the site (Osaka Port)

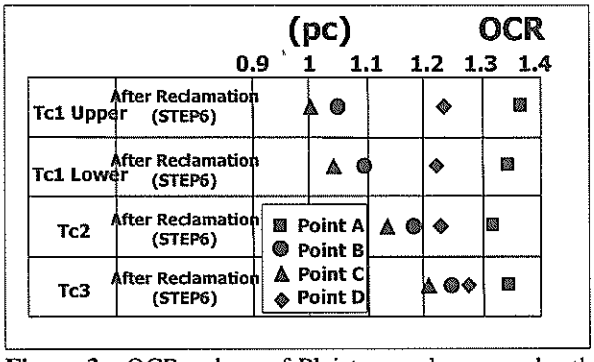

Figure 3 OCR values of Pleistocene layers under the ventilation tower

smaller c_v in the normally consolidation region and to consider the secondary settlements with the coefficient of secondary compression,C_α.

Another example is the Kansai International Airport (KIA) construction project, which was constructed on an artificial island in the Osaka Bay, which is 5 km off the southwest of Osaka City (Arai, 1991;Arrai et al., 1991; Endo et al., 1991). The airport was inaugurated in September 1994, when the first phase of construction was completed. As the airport is being operated with only one runway, the second phase construction project commenced in July 1999, aiming the completion of the second runway parallel to existing one up to 2007.

Figure 4 is the soil profile of the site, showing that the Pleistocene gravel-sand layers and clay layers are accumulated alternately up to 400m depth, and the over-consolidation ratio before the reclamation are 1.0-1.5. When the project was planned in 1970s, most of engineers hardly expected that the settlements of Pleistocene clay layers might make an important problem, because they did not have experiences of large settlements of Pleistocene layer at that time. **Figure 5** shows measured settlement with time at an observation point in KIA, where the largest settlement was observed (Kobayashi,1994). As shown in **Figure 5**, the consolidation settlement of Holocene clay layer improved by sand drain method ended up within 6 months after reclamation, while the settlement of Pleistocene clay layer commenced when the level of reclaimed land reached almost the sea level, and has continued after opening the airport. Recently the total settlements in the island have become larger than 11m and about 5m out of the total settlement is by the settlement of Pleistocene layer.

The reclaimed area in the second phase has an average water depth of 19.5 m, in comparison with 18.0 m in the first phase. The average thickness of the Holocene clay layer in new site location is 24 m (18 m in the first phase), which will increase the volume of reclaimed sand or

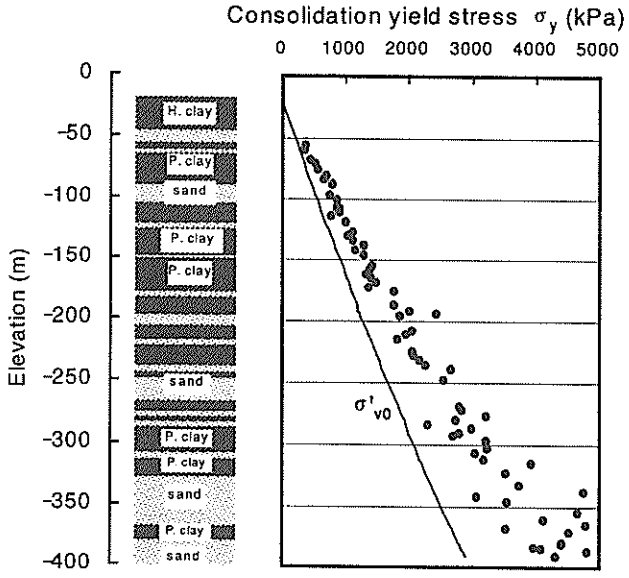

Figure 4 Soil profiles at the site (KIA)

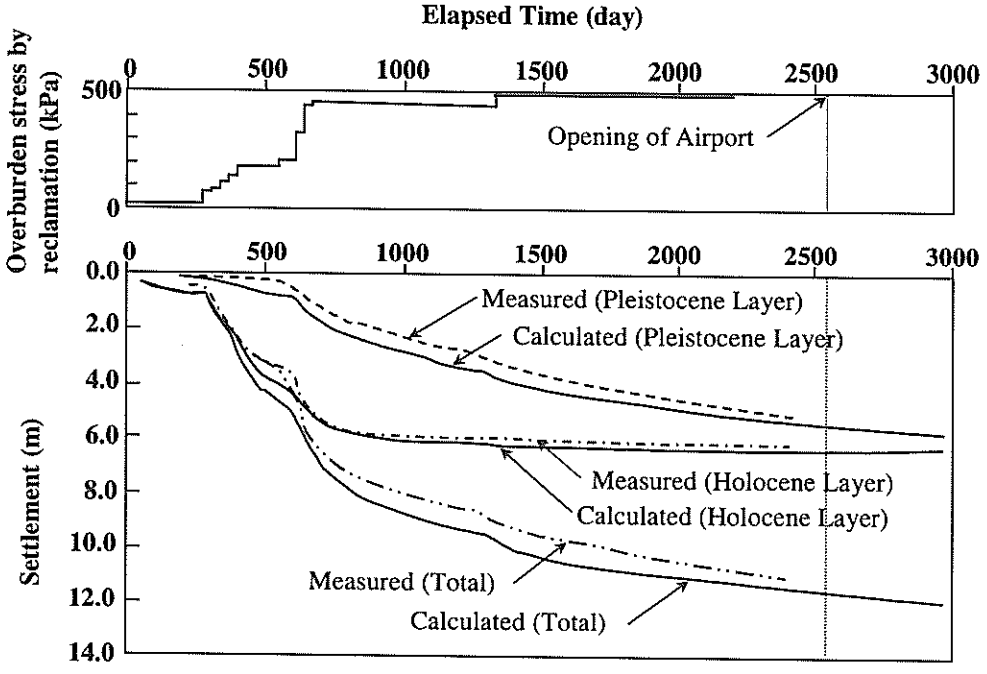

Figure 5 Measured settlement with time in KIA island (Kobayashi, 1994)

gravel by 40%, compared to the first phase. The prediction of settlement in the second phase has been carried out based on the experiences of the first phase and the mean predicted total settlement in the reclaimed island is 18m, which is probably the largest consolidation settlement geotechnical engineers have experienced. Therefore, in the second phase project, both the observation of settlement and the version-up of settlement prediction would be the most important works as the construction control.

The problems of settlement prediction of Pleistocene clay layer in Osaka Bay are summarized as follows:

1) Pleistocene clay layers often show much larger compressibility than Holocene clay layers. The settlement of Pleistocene clay commences sharply when the overburden stress exceeds a critical value, which is not necessarily equal to the consolidation yield stress obtained in laboratory test.
2) Even if the overburden stress is less than consolidation yield stress, large settlements can take place in Pleistocene clay layers. In this case, it seems that the settlement includes both the primary settlement and the secondary settlement, although the distinction is usually difficult.
3) Because Pleistocene clay layer exists at large depth, counter-measures such as ground improvement methods are practically not available and the correct prediction of the behavior is inevitable to design.

The research group in Port and Harbour Research Institute has been carried out intensive studies on mechanical properties of aged clays those have structures formed during the process of long-term sedimentation and consolidation. In the former part of this report, the method for evaluating the degree of structure is newly proposed and a unique consolidation behavior of structured clay is presented. In the latter part, the compression and shear characteristics of aged clay, are reviewed with related to the case study on KIA project.

2 COMPRESSIBILITY OF AGED CLAY AND STRENGTH INCREASE DUE TO CEMENTATION

2.1 Compression index ratio

Bjerrum (1967, 1973) firstly pointed out the importance of structure and aging effect of clay deposits on the mechanical properties. **Figure 6** shows a schematic e-log p relationship proposed by Bjerrum, where the difference between young clay and aged clay was explained by the secondary or delayed consolidation, i.e.; the aged clay was characterized by the increase of consolidation yield stress p_c and the decrease of void ratio due to the secondary consolidation during a long-term sedimentation age.

Another type of the difference in e-log p curve between natural aged clays and reconstituted young clays is frequently seen as shown in **Figure 7**, where e-log p curve has a sharp concave downward for natural clay, while young clay has a gentle e-log p curve. This type of change on e-log p curve cannot be explained by the concept in **Figure 6**. Tsuchida et al (1991) defined a compression index ratio, r_c by the following equation and measured the values of r_c for Japanese marine clays:

$$r_c = C_{cmax}/C_c^* \quad (1)$$

where, C_{cmax} is the peak value of C_c in **Figure 8** and C_c^* is the C_c at which consolidation pressure is 5 times larger than p_c.

Compression index ratio, r_c of Holocene clays are plotted with the plasticity index I_p and clay content in **Figure 9(a).** As shown in the figure, r_c clearly shows the positive

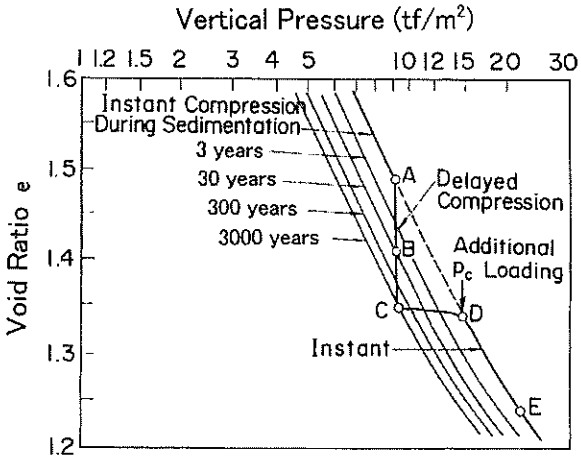

Figure 6 Schematic e-log p relationship during the sedimentation process (Bjerrum,1967)

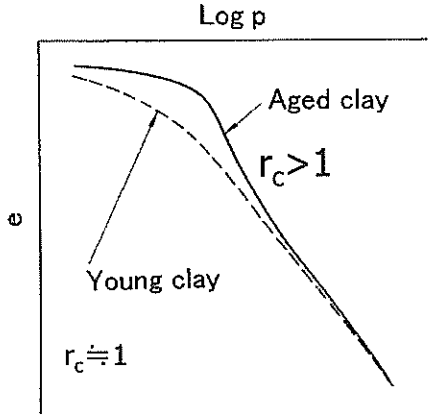

Figure 7 Difference in e-log p curve between aged clay and reconstituted clay

correlation with I_p and clay content. **Figure 9(b)** shows r_c with depth at a site in Osaka Bay, where the landfill was carried out after constructing sand drain. The sampling and soil tests were conducted both before the installation of drain and during the landfill work. As shown in **Figure 9(b)**, r_c of Osaka Bay Holocene clay increased with depth before the installation of drain, however, during the consolidation with the landfill, the r_c became almost constant value near 1.0. According to Tsuchida et al. (1991), the values of r_c of Japanese clays are from 1.1 to 3.0 in Holocene clays and from 1.1 to 6.0 in Pleistocene clays and they usually increases with the depth. On the other hand, the r_c values of reconstituted young clays are almost 1.0.

Figure 10 illustrates a schematic one-dimensional compression curve explaining the effects of cementation and secondary compression. If the consolidation pressure increases until p_0, and ceased at point A for a long time, the void ratio will reduce along the path AB accompanied with secondary compression as explained in **Figure 6**. At the same time, the formation change and chemical alteration will take place among soil particles under conditions not related with the volumetric compression. These changes have the effect of strengthening particle interlocking, namely bonding and will certainly make a contribution to strength gain. In this paper, the component of strength gain not associated with volumetric compression is classified as cementation, in a very broad sense. The cementation includes various factors, such as flocculation, thixotropy, leaching and so on.

When the sample at point B is subjected to additional pressure increase, the natural clay generally shows compression characteristics as shown by curve BCDE. Here, the author define the difference between p_c and p_i as the result of cementation. Based on the distinction, as suggested in **Figure 10,** the compression index ratio, r_c, is an index of the effect of cementation ($p_c - p_i$) and not related to the secondary consolidation ($p_i - p_0$).

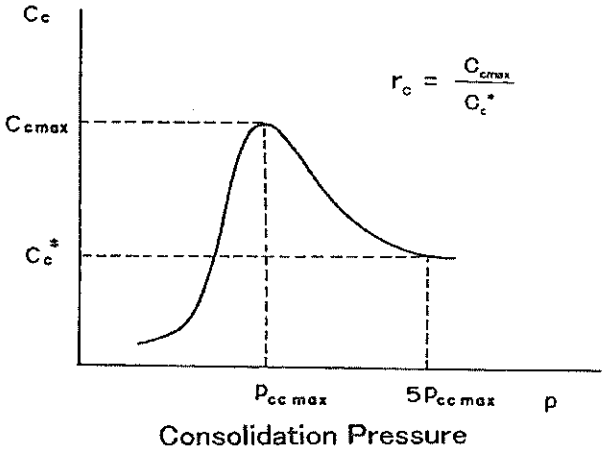

Figure 8 Compression index ratio

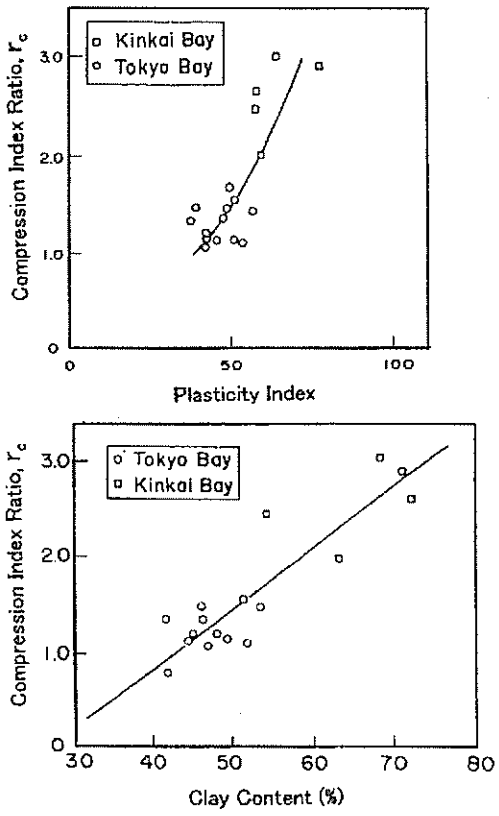

Figure 9(a) Compression index ratio, r_c, with I_p and fine content

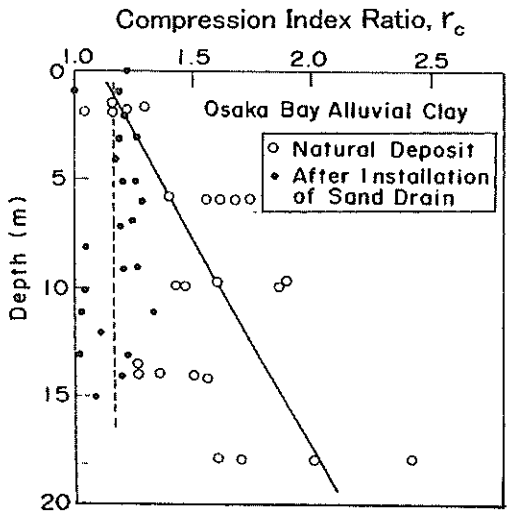

Figure 9(b) Change of r_c after consolidation

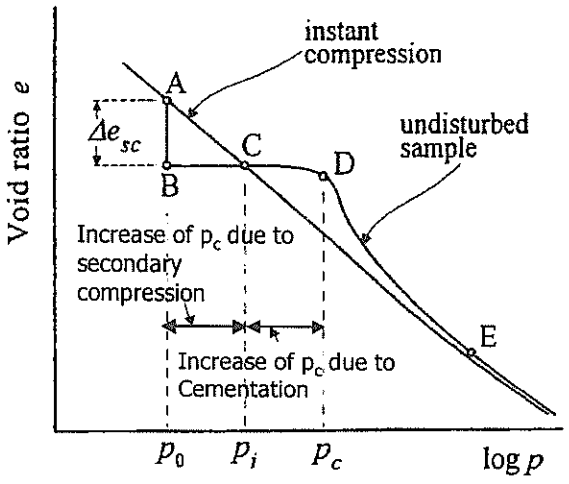

Figure 10 Effect of cementation and secondary compression on e-log p curve

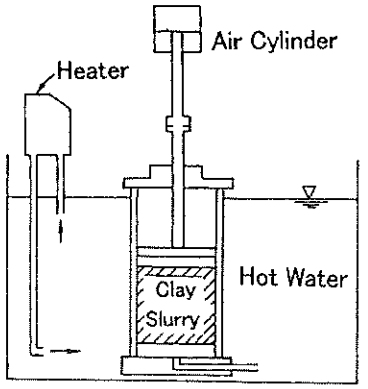

Figure 11 Apparatus of high temperature consolidation

2.2 Duplication of structure by high temperature consolidation

Tsuchida et al. (1991) proposed a method for constructing the structure of aged clay in laboratory, by consolidating remolded clayey slurry under 75° C. This method is called "high temperature consolidation method".

Tokyo Bay clay was thoroughly remolded at a water content more than twice the liquid limit. The slurry was put into a 20 cm diameter consolidation cell and consolidated one-dimensionally. The consolidation cell was surrounded by hot water with the temperature of constant 75° C adjusted by an electric heater as shown in **Figure 11.** Clay was first consolidated under the weight of loading plate and 4 incremental pressures (10, 20, 40, 80 kPa) were applied subsequently by the air cylinder. After the completion of consolidation, the sample was unloaded and cooled down at the room temperature (25° C).

Figure 12 shows a time settlement relationship of sample consolidated under high temperature (HTC), and conventional sample consolidated under room temperature (RTC), for each pressure increment. As shown in the figure, the settlement of HTC under the weight of loading plate was smaller than that of RTC. However, under subsequent loading, the settlement of HTC was larger than that of RTC. Comparing the water contents of both samples after the completion of consolidation, the water content of HTC sample was slightly larger than RTC sample. The consolidation settlement of HTC is obviously accelerated by high temperature condition.

Figure 13 shows the e-log p curve obtained for both HTC and RTC samples, where the e-log p curve of undisturbed Tokyo Bay clay is shown for comparison. As

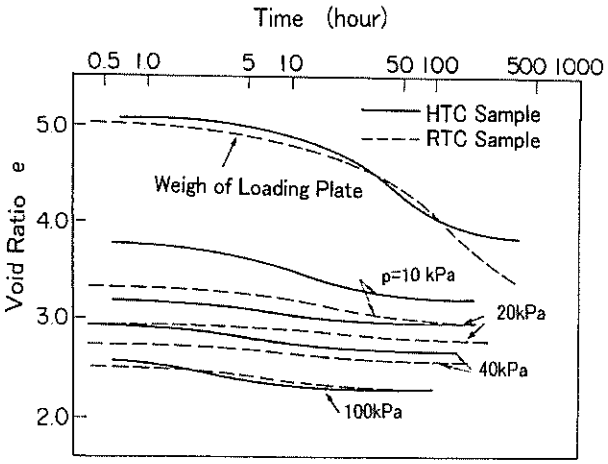

Figure 12 Time settlement relationship under high temperature consolidation

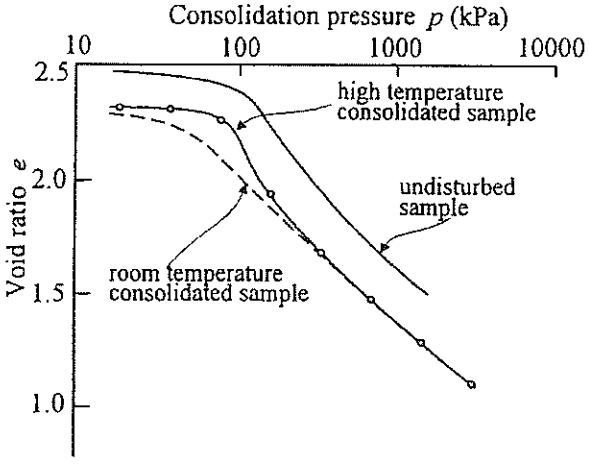

Figure 13 e-log p curves of HTC sample and RTC Sample (Tsuchida et al.,1991)

shown in **Figure 13**, e-log p curve of HTC sample resembles that of undisturbed clay which must have undergone aging for thousands years, showing distinctive yielding and larger compressibility after yielding. As the compression index ratio r_c of HTC sample were 1.9-2.0, it can be said that the procedure of high temperature consolidation is a useful technique to reproduce the structure as Holocene clay deposits have in the laboratory. Based on the concept shown in **Figure 10**, as the water content of HTC sample was slightly larger than RTC sample, it is considered that be the main cause of the acceleration of cementation action will the effect of high temperature consolidation.

Kitazume and Terashi (1994) used a procedure of high temperature consolidation to make a model ground in centrifuge model test of slope stability. **Figure 14** shows comparison of deformation in slope when the model slope failed. As shown in **Figure 14**, the model slope of HTC clay failed suddenly and the deformation was concentrated around a sliding surface, while the model slope of RTC clay failed after large deformation of the whole model slope. It can be said that the slope of HTC clay shows brittle behavior analogous to natural slopes. The procedure of high temperature consolidation is a useful technique to duplicate aged clay in laboratory

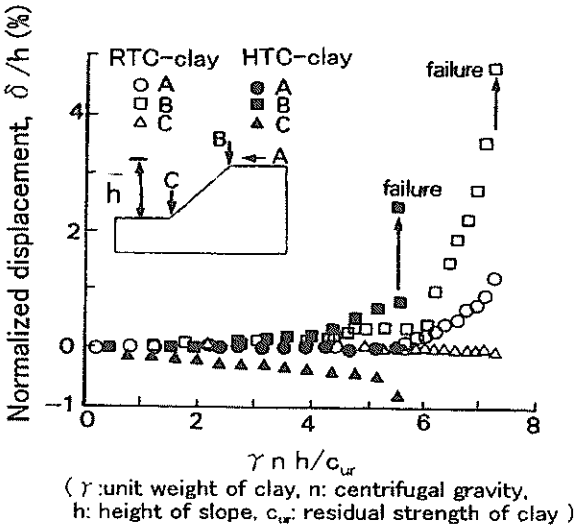

Figure 14 Deformation of slope at failure in centrifuge model test (Kitzume and Terashi,1994)

2.3 Increase of strength due to the cementation effect

As mentioned above in **Figure 10**, the strength gain with time can be divided into two components. One of them is associated with volumetric compression, while the other is attributed to the cementation effect. When the shear strength gain from point A to point B in **Figure 10** are shown as Δs_u, it can be assumed that the strength gain due to the volume decrease will be given as $(s_u/p)\ (p_i - p_0)$, where (s_u/p) is a strength increment ratio of normally consolidated condition. Accordingly, the strength increment due to the cementation is obtained as $(\Delta s_u - (s_u/p)\ (p_i - p_0)$.

Using this assumption, Tan and Tsuchida (1999) investigated the shear strength gain by cementation effect experimentally, and showed that the strength increment by cementation is proportional to elapsed time, and the increment is related to the overburden stress. **Figure 15**

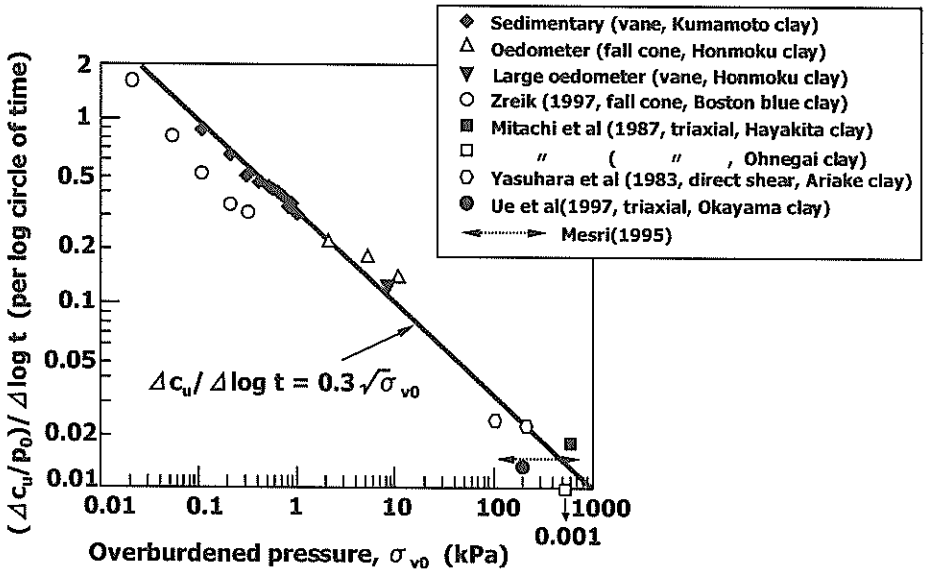

Figure 15 Relationship between normalized strength increment and effective overburden pressure .

shows the relationship between the normalized strength increment per 1 log-scale of time, $(\Delta s_u/p)/\Delta \log t$, and the effective overburden pressure p. As shown in Figure, the strength increment can be expressed by the following simple equation;

$$(\Delta s_u/p)/\Delta(\log t) = 0.3/\sqrt{p} \qquad (2)$$

or $$\Delta s_u = 0.3\sqrt{p}\,\Delta(\log t) \qquad (2)'$$

where, p is an overburden pressure (unit: kPa), and t is an elapsed time after the end of primary consolidation.

Equation (2) and (2)' mean that the strength increment by cementation is proportional to $\sqrt{p}$ and $\Delta(\log t)$, accordingly, the contribution of cementation dominates strength gain with time when the overburden pressure is smaller than 100kPa, while strength gain due to secondary compression becomes the main component when the overburden pressure is larger than 100kPa.

3 EVALUATION METHODS OF STRUCTURE OF AGED MARINE DEPOSITS

3.1 Ultimate Standard Compression Curve (USC)

In the previous sections, the mechanical properties of aged clay have been examined experimentally. In the practical sense, it seems that the method to evaluate the degree of the structure quantitatively is necessary. Recently the author has proposed a concept of standard compression curves (SCC) for marine clays to explain the various aspects of e-log p relationship of clays in a unified manner. Here the SCC concept is introduced and it is shown that the degree of structure of marine deposits can be easily evaluated, using the SCC concept.

A number of studies have been carried out on the e-log p relationship of clays. An early study by Skempton (1944) showed the following fundamental findings;

a) Compressibility index, C_c has a strong relationship with the liquid limit w_L.
b) Sample disturbance of natural clay and the initial water content of laboratory-prepared clay have important effects on the e-log p relationship.
c) There exists some discrepancy between the laboratory compression curve and the sedimentation compression curve, which is obtained as the relationship between in-situ void ratio and the overburden stress in geologically normally consolidated layer.

The empirical relationship between C_c and w_L has been studied by a lot of researchers. Terzaghi and Peck (1969) proposed the well-known equations based on the experimental data by Skempton as follows;

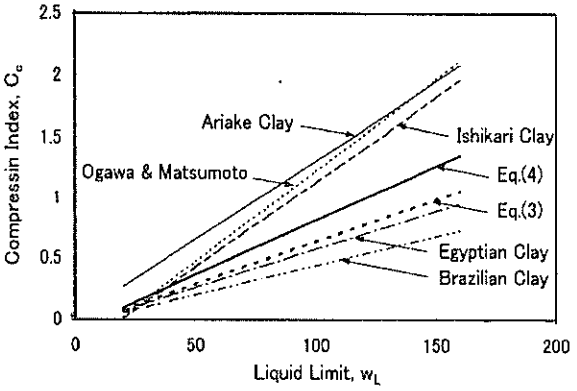

Figure 16 Comparison of empirical equations on C_c-w_L relation

$$C_c = 0.007\,(w_L - 10) \quad \text{for remolded soil} \qquad (3)$$

$$C_c = 0.009\,(w_L - 10) \quad \text{for undisturbed soil} \qquad (4)$$

However, as the above equations do not always give good estimation of C_c especially for undisturbed soils, various empirical equations for different clays have been proposed as follows:

$C_c = 0.015(w_L - 19)$, for Japanese marine clays (Ogawa and Ogawa, 1978)
$C_c = 0.014(w_L - 20)$, for Ishikari clay (JSSMFE, 1966)
$C_c = 0.013\,w_L$, for Ariake clay, (JSSMFE, 1966)
$C_c = 0.0063(w_L - 10)$, for Egyptian clay (Abdrabbo and Mahmoud, 1990)
$C_c = 0.0048(w_L - 10)$, for Brazilian clays, (Bowles, 1979)

Figure 16 shows the comparison of above equations. Looking at **Figure 16**, a question arises such as "why is the compressibility of natural soil so much different among the soil types?". The concept of standard compression curve is to provide a unified model to explain the compressibility of different clays with a few fundamental parameters, such as, liquid limit, sensitivity and initial void ratio.

Let us consider some typical characteristics of e-log p curves of clays. **Figure 17(a)** is e-log p curve of reconstituted Osaka Bay clay, showing a typical linear relationship between void ratio e and log p, while **Figure 17(b)** is e-log p curve of undisturbed sample of Osaka Bay Pleistocene clay. As mentioned in Chapter 2, in cases of these structured clays, e and the log p are not linear in normally consolidation region.

Figure 17(c) shows the change of e-log p curves due to the sample disturbance (Okumura, 1974). As shown in **Figure 17(c)**, when the clay sample is disturbed or is given some shear strain before the consolidation, the bending of e-log p curve at consolidation yield stress becomes obscure and the void ratio decreases as a whole by the disturbance. **Figure 17(d)** is e-log p curve of Kumamoto Port clay, which is consolidated carefully from slurry of 400% water content to the maximum consolidation pressure of 1Mpa. As shown in **Figure 17(d)**, the e-log p curves from p=0.01 kPa to 1 Mpa is not linear but shows a convex to the bottom. It has been known that e-log p curve is not linear when clay is consolidated from the extremely high water content condition (Imai,1982).

In **Figures 18(a),(b),(c)** and **(d),** the same data in **Figure 17(a),(b),(c)** and **(d)** are plotted in ln f –log p system, respectively, where f is a specific volume of soil and equal to $(1+e)$, and ln and log mean natural and common loga-

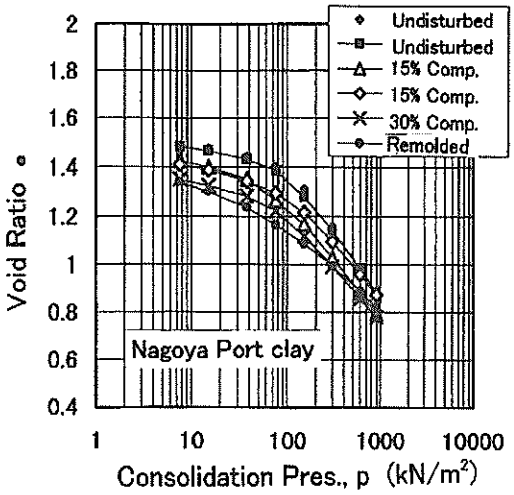

Figure 17(c) Change of e-log p curve due to sample disturbance

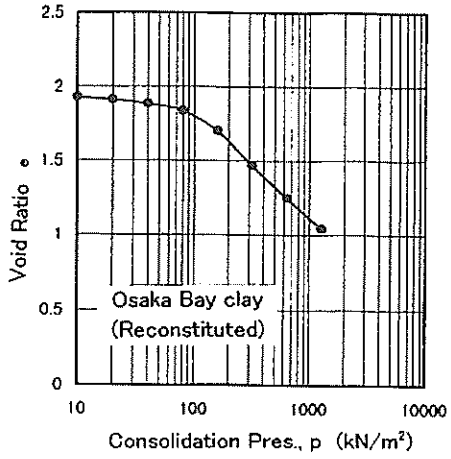

Figure 17(a) e-log p curve of reconstituted Osaka Bay Clay

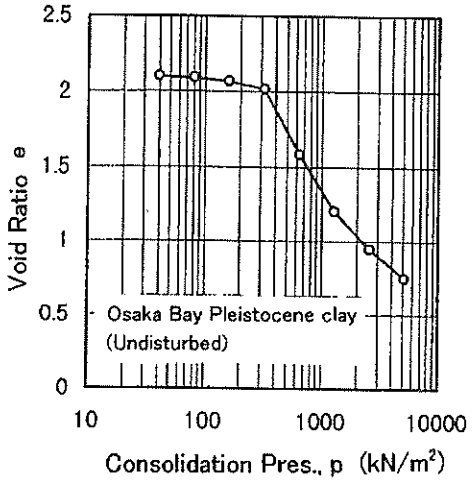

Figure 17(b) e-log p curve of undisturbed Pleistocene clay

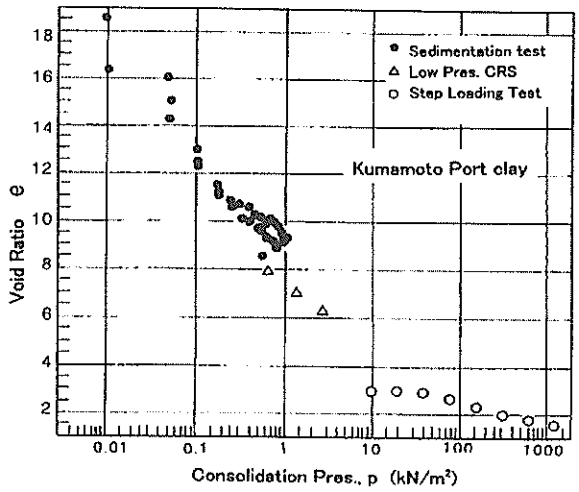

Figure 17(d) e-log p curve of clay with high water content

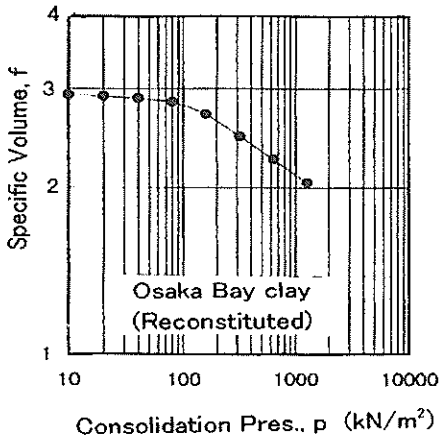

Figure 18(a) ln f-log p curve of reconstituted Osaka Bay clay

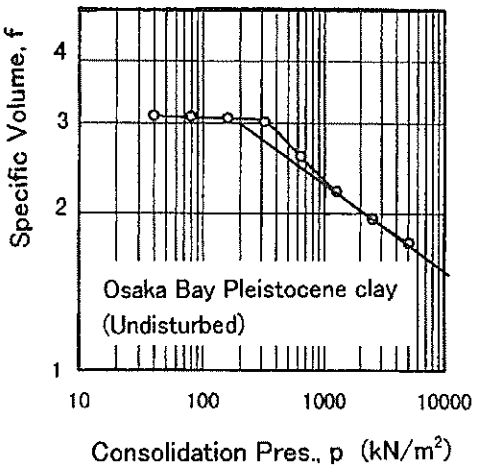

Figure 18(b) ln f-log p curve of undisturbed Pleistocene clay

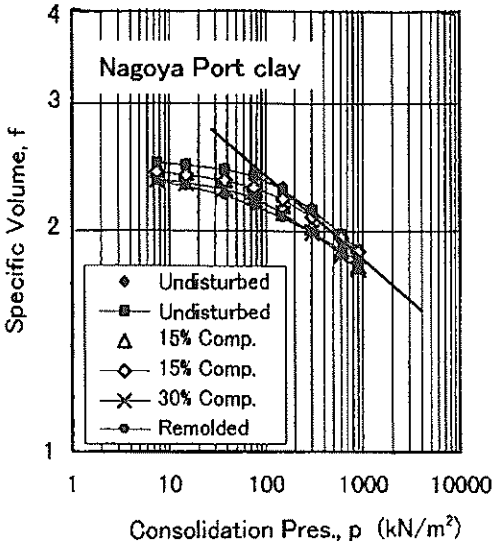

Figure 18(c) ln f-log p curve of disturbed sample

rithm, respectively. In **Figure 18(d)**, the linearity between ln f and log p is recognized as a whole, and in **Figures 18(a),(b)** and **(c)**, ln f - log p seems to be close to a straight line as the consolidation pressure increases.

Summarizing **Figures 17** and **Figures 18**, the followings are obtained;

- The linearity between e and log p is not commonly recognized, depending on the existence of structure, sample disturbance and initial water contents.
- However, in all 4 cases, focusing on the relation where the consolidation pressure is large enough, a linearity between ln f and log p seems to exist. This is because the effects of the structure, disturbance and initial void ratio will disappear with the increase of consolidation pressure.

Based on the above considerations, the following assumption on the existence of Ultimate Standard Compression Curve (USC) is made;

a) When clay is consolidated one-dimensionally from slurry with large initial void ratio, it shows the linear relationship between ln f (=1+e) and log p. This curve is named Ultimate Standard Compression Curve (USC), and it can be determined mainly by the liquid limit of clay.

b) In case that natural sedimentary clay has a structure due to aging, the void ratio e_0 can be larger than the value given by USC. When natural clay sample is consolidated after it is disturbed or remolded with an void ratio, its void ratio becomes smaller than the value given by USC,

c) By consolidating clay samples with the consolidation pressure much larger than the consolidation yield stress p_c, the effect of structure due to aging and the effects of the sample disturbance or initial void ratio dis-

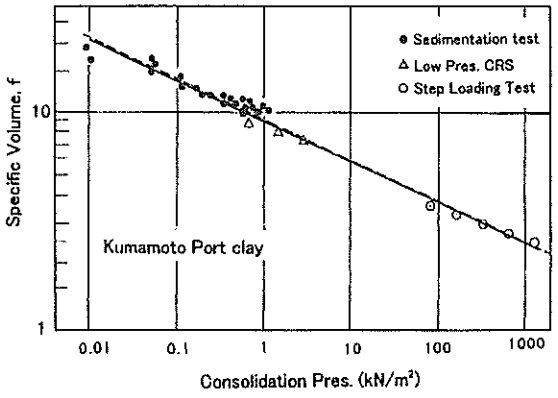

Figure 18(d) ln f-log p curve of clay with high water content

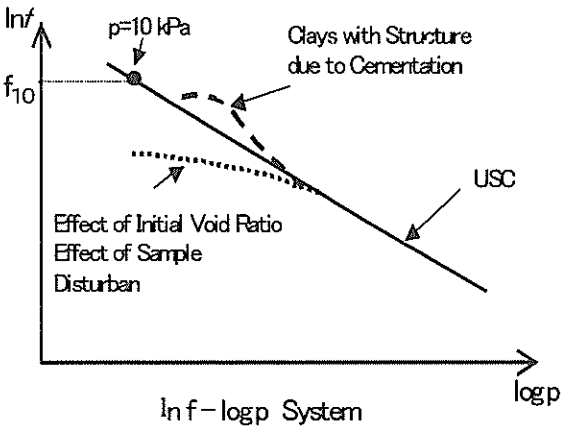

Figure 19 Ultimate standard compression curve, USC

appear, and finally the e-log p relation converges into USC.

Figure 19 illustrates the USC concept in the log f - log p system. USC can be described by the following equation;

$$\ln f = -C(\log p - 1) + \ln f_{10} \quad (5)$$

where, f is specific volume and equal to the void ratio e plus 1, f_{10} is the specific volume when p=10 kPa on the standard curve. C is a gradient of USC, given by the compression index C_c and e as follows;

$$C = C_c / (1 + e) \quad (6)$$

C is the parameter called compression ratio (Terzaghi and Peck,1967). Butterfield (1979) firstly proposed the linearity between ln f and log p as shown in Eq.(5). By the differentiation of Eq.(5), the following is obtained;

$$df/f = -0.434\, C\, (dp/p) \quad (7)$$

df/f is a natural strain of soil, while dp/p was named *natural stress* by Butterfield (1979), who pointed out that, Eq.(5) expressing linearity between natural strain and natural stress, will be a fundamental law of geo-materials.

3.2 Existence of a unique USC determined by liqiud limit

To study the validity of the existence of USC, 725 consolidation test data of 18 marine deposits listed in **Table 2** were analyzed by the following procedure:

1) To plot the specific volume f and the consolidation pressure p in ln f–log p system.
2) To ascertain the linearity between ln f and log p in the region that p is 2 times larger than the consolidation yield stress p_c, and to determine the straight line (USC) for ln f - log p relation.
3) To calculate the compression ratio, C ,and the specific volume on USC when p=10kN/m^2, f_{10}.

Table 1. List of Data of Consolidation Tests

Clay	Number of Data	Liquid limit w_L (%)
1. Haneda,Japan	270	31.1 - 125.0
2. Yokohama Port, Japan	67	54.7 - 129.9
3. Kasumigaura,Japan	51	66.9 - 205.0
4. Sakata Port, Japan	14	63.1 - 102.8
5. Osaka Bay Holocene, Japan	56	48.8 - 117.7
6. Osaka Bay Pleistocene, Japan	58	40.4 - 138.0
7. Hachirogata, Japan	12	94.6 - 225.6
8. Kuwana, Japan	16	50.3 - 92.1
9. Maizuru, Japan	27	33.0 - 91.6
10.Kinkai Bay Japan	17	53.5 - 112.9
11.Tamano, Japan	7	52.0 - 92.5
12.Izumo, Japan	12	61.6 - 138.0
13.Ariake, Japan	38	54.5 - 137.4
14.Banjarmasin, Indonesia	27	76.8 - 137.4
15.Singapore	19	50.5 - 82.3
16.Bankok, Thailand	10	45.8 - 99.6
17.Drammen, Norway	14	31.6 - 55.2
18.Bothkenar, United Kingdom	10	55.2 - 76.9

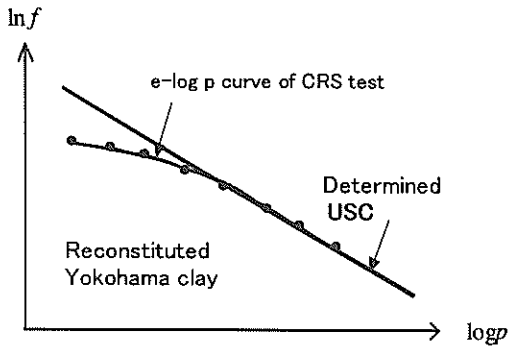

Figure 20(a) ln f – log p relationship and determination of USC (Yokohama Clay)

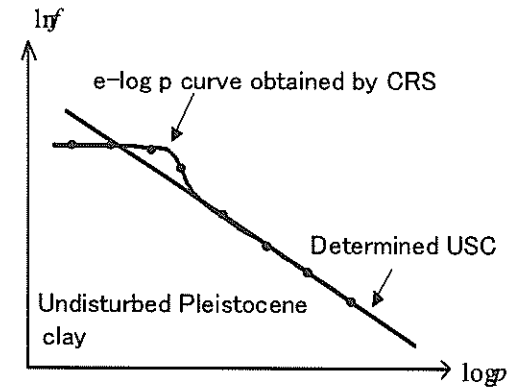

Figure 20(b) ln f – log p relationship and determination of USC (Osaka Bay Pleistocene Clay)

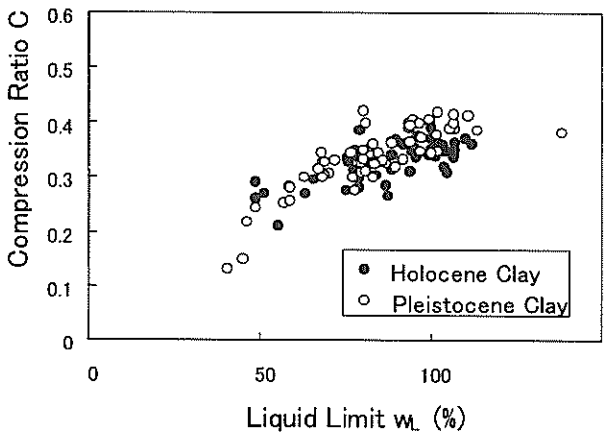

Figure 21(a) C - w_L relationship (Osaka Bay clay)

Figure 20(a) and **Figure 20(b)** are the $\ln f - \log p$ relationships of Reconstituted Yokohama clay and Undisturbed Osaka Bay Pleistocene clay, which were obtained by the constant rate strain consolidation tests, respectively. In both figures, when the consolidation pressures are 3 - 4 times larger than the consolidation yield stress, the linearity of $\ln f$ and $\log p$ were observed. The determination of USC was made with the regression analysis of data of these range. In Yokohama Clay, the specific volume f was smaller than USC in all the range of consolidation pressure, however, in Osaka Bay Pleistocene Clay, the specific volume was larger than USC when the p was close to p_c, and with increase of the consolidation pressure, the $\ln f$-$\log p$ relationship con-verged to the USC.

Figure 21(a) and **Figure 21(b)** are the relationships be-

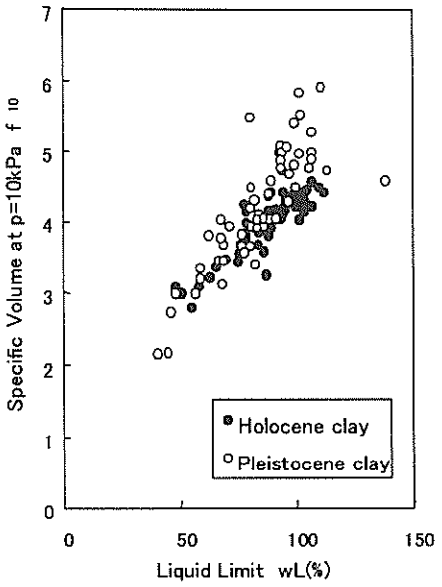

Figure 21(b) f_{10} - w_L relationship (Osaka Bay clay)

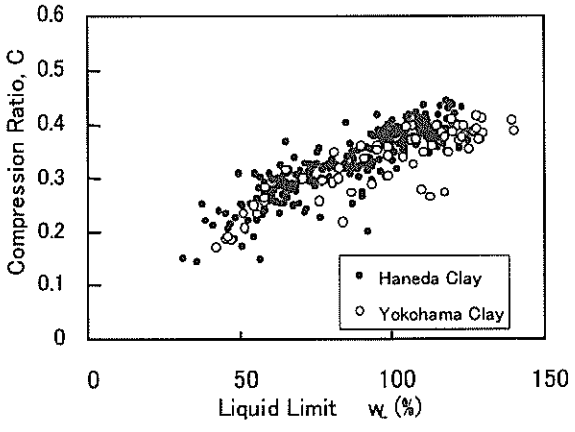

Figure 22(a) C-w_L relationship (Haneda clay and Yokohama clay)

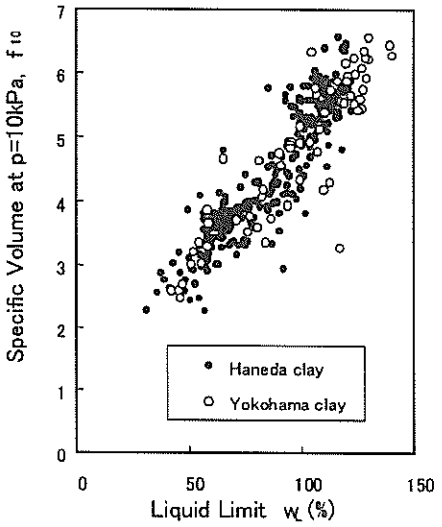

Figure 22(b) f_{10}-w_L relationship (Haneda clay and Yokohama clay)

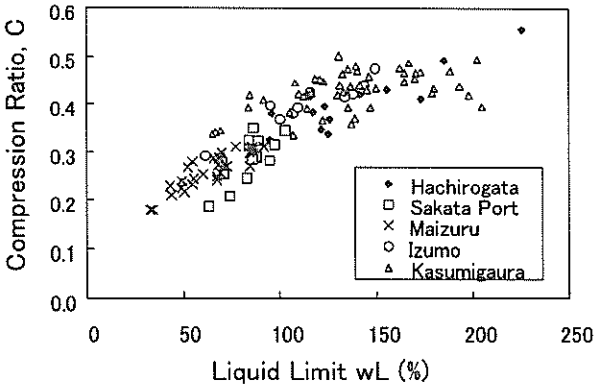

Figure 23(a) C-w_L relationship (Hachirogata, Sakata Port, Kasumigaura, Maizuru Port and Izumo clays)

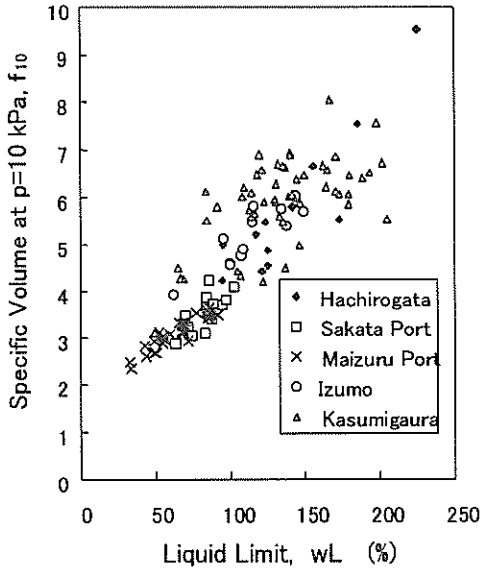

Figure 23(b) f_{10}-w_L relationship (Hachirogata, Sakata Port, Kasumigaura, Maizuru Port and Izumo clays)

tween C and w_L, f_{10} and w_L of Osaka Bay Holocene and Pleistocene clays, respectively. As shown in the figures, both C and f_{10} increase with the liquid limit and the correlation is fairly good. These results are seen in other marine clay. **Figure 22(a)** and **Figure 22(b)** are $C - w_L$ and $f_{10} - w_L$ relationships of Haneda clay and Yokohama clay, located in Tokyo Bay area. The relations are similar to those of Osaka Bay clay.

Figure 23(a) and **Figure 23(b)** are the same figures of Hachirogata clay, Sakata clay, Maizuru clay, Izumo clay and Kasumigaura clay, which are located at coastal area facing to Japan Sea or Kasumigaura Lake. **Figure 24(a)** and **Figure 24(b)** are the same figures of Kinkai clay, Tamano clay, Ariake clay and Kuwano clay, which are located at coastal area in Western Japan. The results for non-Japanese clays, such as Indonesia, Scotland, Norway, Singapore and Thailand, are shown in **Figure 25(a)** and **Fig-**

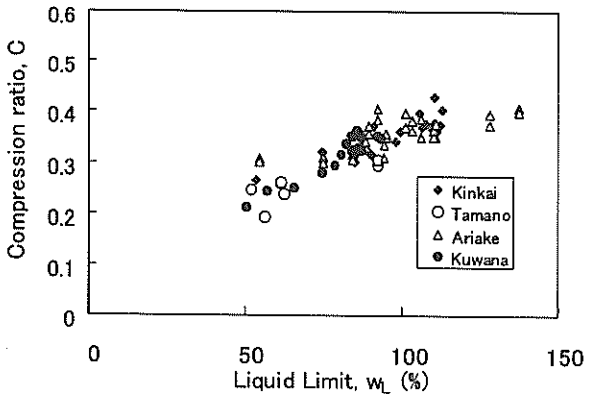

Figure 24(a) C-w_L relationship (Kinkai Bay, Tamano, Ariake and Kuwana clays)

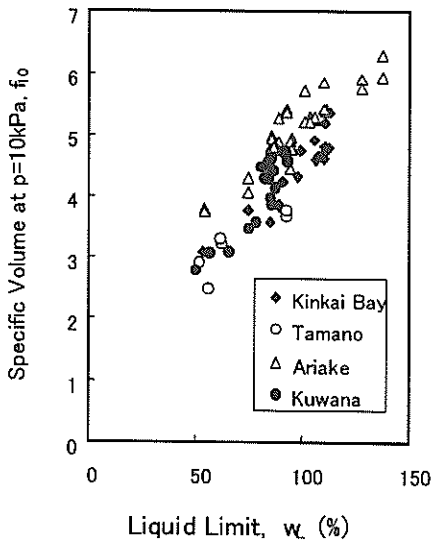

Figure 24(b) f_{10}-w_L relationship (Kinkai Bay, Tamano, Ariake and Kuwana clays)

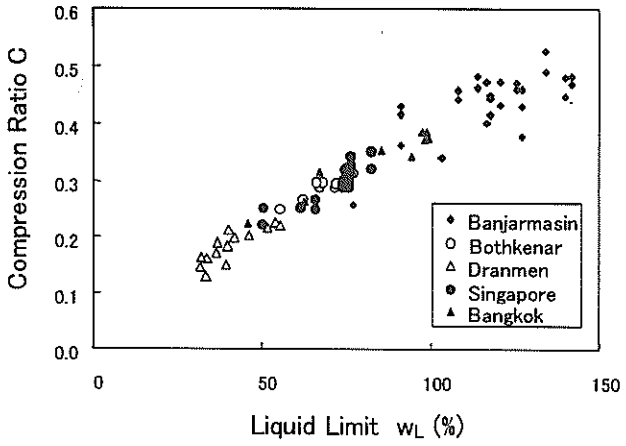

Figure 25(a) C-w_L relationship (Banjarmasin, Bothkenar, Drammen, Singapore and Bangkok clays)

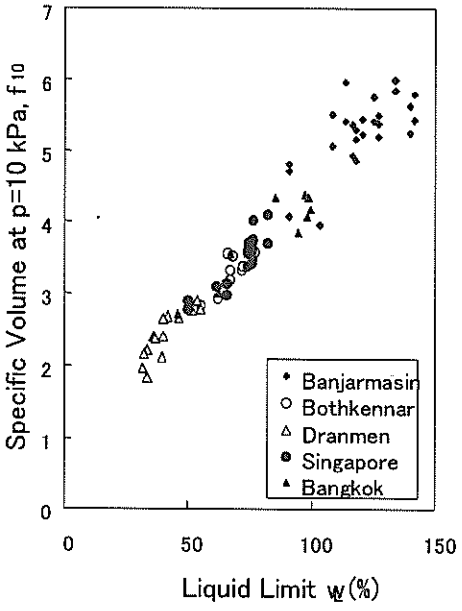

Figure 25(b) f_{10} - w_L relationship (Banjarmasin, Bothkenar, Drammen, Singapore and Bangkok clays)

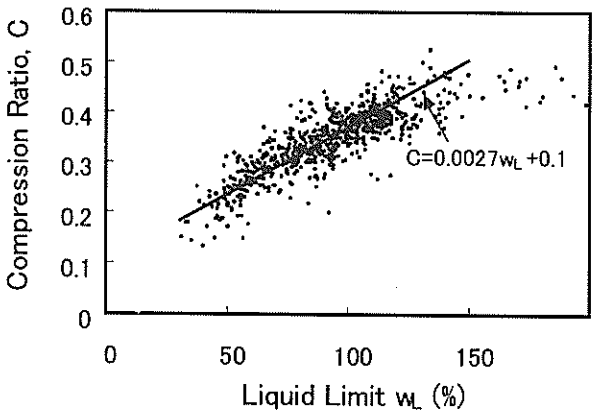

Figure 26 C— w_L relationship (all data)

ure 25(b). In all these figures, common relationship is observed.

Figure 26 and **Figure 27** are C-w_L relation and f_{10}-w_L relation of all of 18 marine clays, respectively. As shown in the figures, both C and f_{10} correlated with w_L fairly well, and the assumption that the USC is determined mainly by the liquid limit of soil seems to be valid for these marine clays. The regression analyses gave the following equations for C and f_{10}:

$$C = 0.0027\, w_L + 0.1 \tag{8}$$

$$f_{10} = 0.042\, w_L + 0.55 \tag{9}$$

USC is the e-p relationship, where the e-p curves converge ultimately with the increase of consolidation pressure. Using Eqs.(8) and (9) with Eq.(5), USC is given by w_L as follows:

$$\ln f = -(0.0027 w_L + 0.1)(\log p - 1) + \ln(0.042 w_L + 0.55) \tag{10}$$

Here we consider the interrelationship between USC concept and the $C_c - w_L$ relations. Conventionally, C_c is determined as the maximum value of $\Delta e / \Delta(\log p)$ in normally consolidation region.

On $C_c - w_L$ relationship of undisturbed clays, Eq.(4) by Terzaghi and Peck (1967) is well-known, while the following equation by Ogawa and Matsumoto(1978) is often referred for Japanese marine clays;

$$C_c = 0.015(w_L - 19) \tag{11}$$

Figure 28 present $C_c - w_L$ relationship of Osaka Bay Clay and Haneda Clay, C and f_{10}, of which are plotted in **Figure 21** and **Figure 22**, respectively. As shown in Figures, Eq.(11) is fitting the data well and Eq.(4) is giving a lower boundary of C_c. Instead of C_c as the maximum value of $\Delta e / \Delta(\log p)$, C_{c1000}, which is $\Delta e / \Delta(\log_{10} p)$ at the consolidation pressure p = 1000 kPa, were calculated and plotted with w_L in **Figure 29**. The relationship between C_{c1000} and w_L is approximated well by Eq.(4).Using the concept of USC, C_{c1000} is the compressibility on USC at

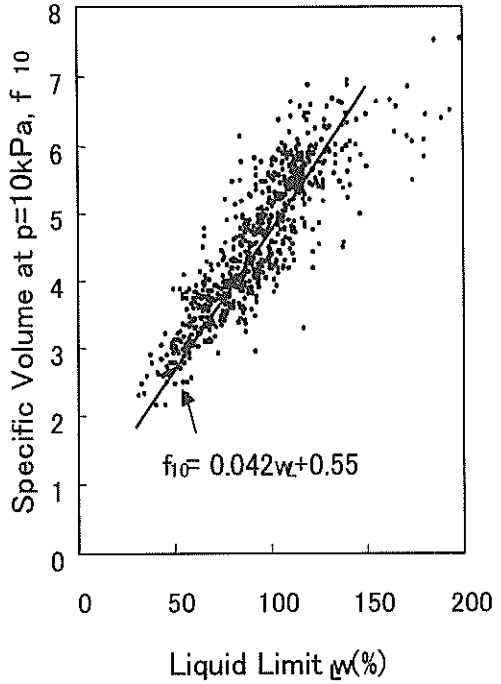

Figure 27 f_{10} – w_L relationship (all data)

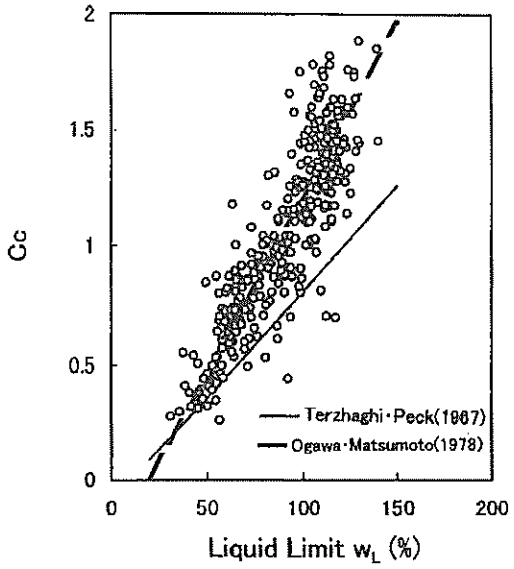

Figure 28 C_c – w_L (Haneda and Osaka Bay clays)

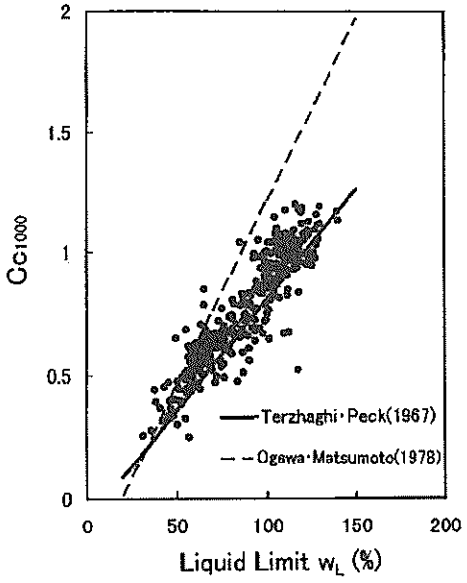

Figure 29 C_{c1000} – w_L (Haneda and Osaka Bay clays)

p=1000kN/m^2, which does not include the effect of structure of aged clay. On the other hand, when the clay has a structure due to the aging, C_c obtained as the maximum value of $\Delta e/\Delta(\log p)$ become lager than C_{c1000}. Accordingly, the difference between Eq.(4) and Eq.(11) may be explained as follows:

$C_c = 0.009\ (w_L - 10)$: for undisturbed soil *without* structure due to aging

$C_c = 0.015(w_L - 19)$: for undisturbed soil *with* structure due to aging

3.3 Normalization of USC on liquid limit of clays

In **Figure 30** and **Figure 31**, instead of water content at liquid limit, w_L , C and f_{10} are plotted to the specific volume at liquid limit , f_L ., respectively. As shown in Figures, the following equations are obtained by the regression analysis:

$$C = 0.27 \ln f_L \tag{12}$$

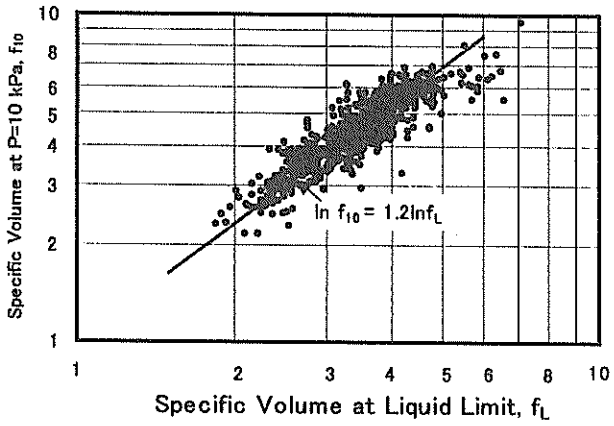

Figure 30 $C - \ln f_L$ relationship (all data)

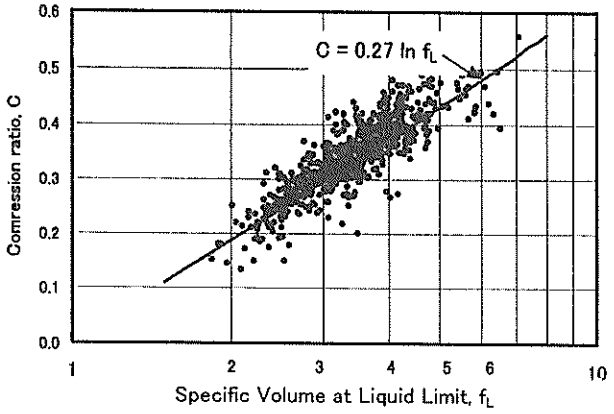

Figure 31 $f_{10} - f_L$ relationship (all data)

$$\ln f_{10} = 1.20 \ln f_L \tag{13}$$

Using Eqs(12) and (13) with Eq.(5):

$$\ln f = -0.27(\ln f_L)(\log p) + 1.20 \ln f_L \tag{14}$$

Dividing both terms by $\ln f_L$:

$$\frac{\ln f}{\ln f_L} = -0.27 \log p + 1.47 \tag{15}$$

Here a specific volume index I_{sv} is newly introduced to normalize specific volume of different soils on the liquid limit. I_{sv} is defined as follows;

$$I_{sv} = \ln f / \ln f_L \tag{16}$$

Using the specific volume index, USC is simply given by;

$$I_{sv} = -0.27 \log p + 1.47 \tag{17}$$

Although it has been known empirically that the liquid limit of clay is a useful index for the compressibility of clay, there seems to be no theoretical explanation why the compressibility of clay is determined mainly by liquid limit of clay. Using the USC concept with Eq.(17), the interpretation can be given as follows:

Figure 32 shows USC by Eq.(17) in I_{sv}- log p system. As shown in figure , I_{sv} is equal to 0, i.e.void ratio of clay is equal to 0, when p=280MN/m^2 on USC (point X). The pressure of 280MN/m^2 is close to the rupture strength of soil particle, such as quarts, feldspar and limestone (Yashima, 1986). Therefore, I_{sv}= 0 at p=280MPa on USC means the ultimate state that voids cannot exist in soil because of rupture of soil skeleton. This consideration is supported by some experimental data. The ln f-log p curves in high-pressure range are shown in **Figure 33**, which are the data of Osaka Bay Pleistocene clay in

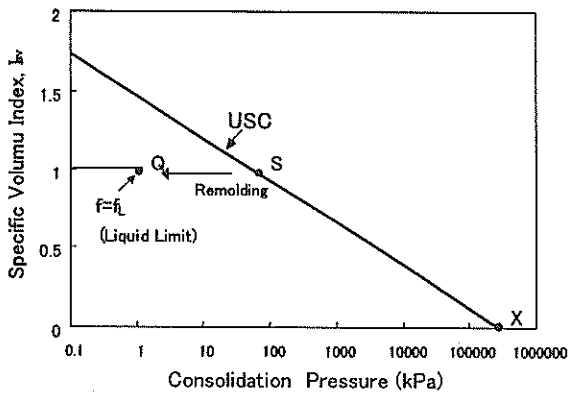

Figure 32 USC in I_{sv} – log p system

CRS(constant rate of strain) consolidation test up to the maximum pressure from 30MN/m^2 to 50M N/m^2 of consolidation pressure. By extrapolating ln f-log p curves of high pressure range, it seems that the void ratios finally become near zero when the consolidation pressure reaches 200 — 400M N/m^2.

In **Figure 32**, the consolidation pressure p_s =55kN/m^2 on USC, when $f = f_L$ and I_{sv}=1 (point S in **Figure 32**). At a void ratio of liquid limit, the shear strength in thoroughly remolded (point Q in **Figure 32**), $(s_u)_{LL}$, ranges from 1.0 to 2.0kN/m^2 (JSSMFE,1992). As the shear strength of point S is given by $(s_u/p)_{USC} \cdot p_s$,where $(s_u/p)_{USC}$ is strength increment ratio on USC, the sensitivity, s_t , at the liquid limit is given:

$$s_t = (s_u/p)_{USC} \cdot p_s / (s_u)_{LL} \quad (18)$$

Using typical values, for example, $(s_u/p)_{USC}$ = 0.25 - 0.35 and $(s_u)_{LL}$ =1.0 - 2.0kPa, the calculated sensitivity s_t for p_s =55kPa ranges from 7 to 19, which agrees well with measured values of typical marine clays. When the sensitivity at liquid limit and strength increment ratio on USC are given, p_s at the point S is determined by:

$$p_s = (s_u)_{LL}\, s_t / (s_u/p)_{USC} \cdot \quad (18)'$$

USC is given by Point X and Point S in **Figure 32**, and the former is related to the rapture strength of soil particles, and the latter is related to the sensitivity at liquid limit and the strength increment ratio on USC. If we assume that both parameters are almost constant in different marine clays, it can be understood that USC is determined mainly by the liquid limit of soil.

3.4 Standard Compression Curve from an initial void ratio SCC(e_0)

In most of clay samples, consolidation pressure p has to be increased to as much as 2-4 times larger than p_c in order that the e-log p curves converge into the USC, as shown in **Figure 19**.When the p is not large enough, the void ratio e is larger or smaller than USC due either to the effect of structure or to the effect of low initial void ratio. Especially, in the range of small consolidation pressure, the effect of low initial void ratio is important.

Figure 34 is a typical e-log p curve of remolded clay of different initial void ratios, e_0. As the initial void ratio is getting larger, the void ratio according to the same consolidation pressure is shifting upper direction, however, all the curves finally converge into a unique line of USC with increase of pressure. The standard compression curve from an initial voids ratio, e_0, is called SCC(e_0) in this study. SCC(e_0) is the e-log p relationship, in the case that the consolidation starts at an initial void ratio e_0* and finally converges into USC with the increase of consolidation pressure.

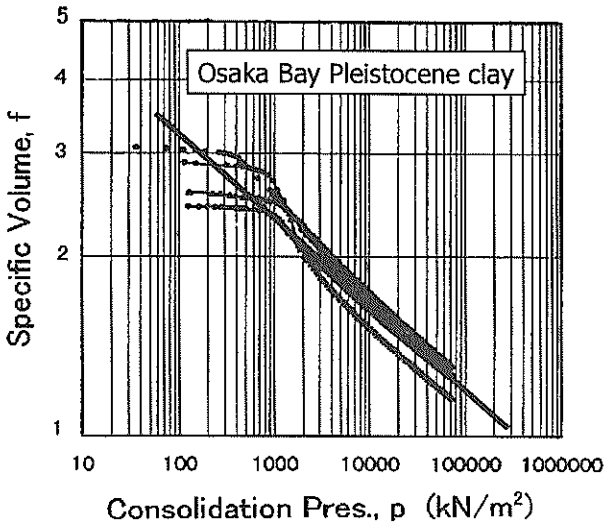

Figure 33 f-log p relationship of Osaka Bay clays obtained by high pressure consolidation test

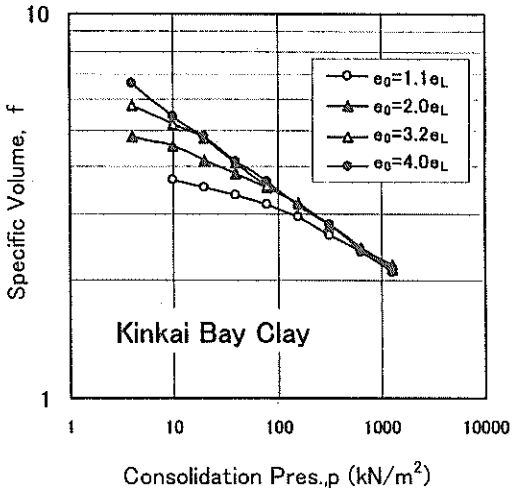

Figure 34 Typical e-log p curve of remolded clay of different initial void ratios

Here, the author induces the SCC(e_0), based on the USC concept and the experimental study on sample disturbance by Okumura (1974).

It is considered that the remolding is an ultimate condition of sample disturbance, and the small amount of effective stress remains after remolding (Okumura, 1974). **Figure 35** shows effective stress change when clay of an initial specific volume f_0 (void ratio e_0) is remolded thoroughly (point B → point A) and is consolidated one-dimensionally. The effective stress condition at Point A is obtained as follows:

Figure 36(a) is the relationship between remolded shear strength c_{ur} and the water content w of clays of different liquid limits. For a give liquid limit, log c_{ur} – log w plot can be expressed by a straight line in a wide range of cur from 10^{-3} kN/m^2 to 10k N/m^2 (Tsuchida et al., 1999). **Figure 36(b)** shows the relationship between s_{ur} and normalized water content w/w_L of the same data. It can be seen that s_{ur} linearly decreases with increase of w/w_L with a relatively narrow band in the bilogarithmic plot. The line of best-fit line is obtained as:

$$s_{ur} = 1.4(w/w_L)^{-4.5}$$

Using the above equation, the strength of Point A in **Figure 35**, s_{uA} ,is given as follws;

$$s_{uA} = 1.4\,(e_0/e_L)^{-4.5} \tag{19}$$

When the strength increment ratio in thoroughly remolded condition is given as $(s_u/p)_{REM}$, the effective stress at point A, p_A , is determined as follows:

$$p_A = s_{uA} / (s_u/p)_{REM}$$

$$= 1.4\,(e_0/e_L)^{-4.5} / (s_u/p)_{REM} \tag{20}$$

Measured values of $(s_u/p)_{REM}$ for some marine clays ranges from 0.8 to 1.2 (Mikasa ,1988)

Point B in **Figure 35** is the effective stress condition of clay of f_0* at the normally consolidated condition on USC. From Eq.(17), the effective stress at point B, p_B, is given as follows;

$$\log p_B = (1.47 - I_{sv0})/0.27 \tag{21}$$

$$p = 10^{(5.44-3.7I_{sv0})} \tag{22}$$

where, I_{sv0} = is a specific volume index of the initial condition and given as $\ln f_0 / \ln f_L$.

According to the comprehensive study on sample disturbance by Okumura (1974), the effect of the sample disturbance on e-log p relationship can be evaluated by disturbance ratio R, which is defined as the ratio of the intact effective stress to the residual effective stress after disturbance or remolding. In this case, R is the ratio p_B/p_A and given as follows;

$$R = \frac{p_B}{p_A} = \frac{10^{(5.44-3.7I_{sv0})}\,(s_u/p)_{REM}}{1.4\,(e_0/e_L)^{-4.5}} \tag{23}$$

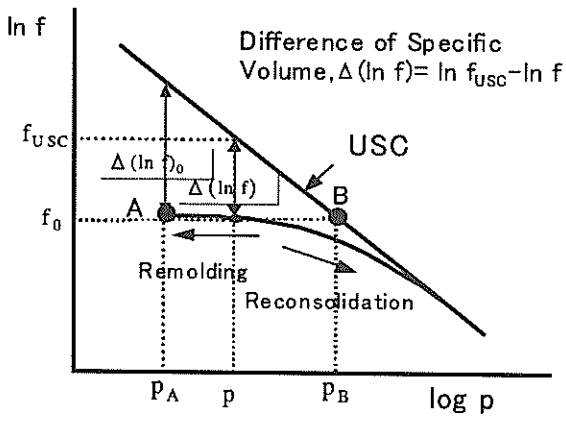

Figure 35 Standard compression curve and effective stress condition of remolded clay

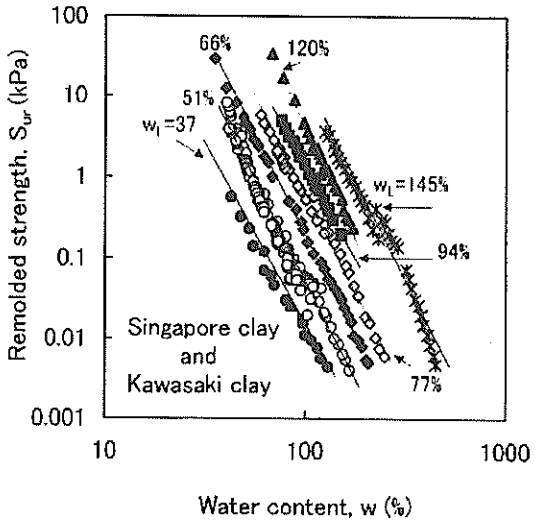

Figure 36(a) Relationship between shear strength of remolded clay and water content

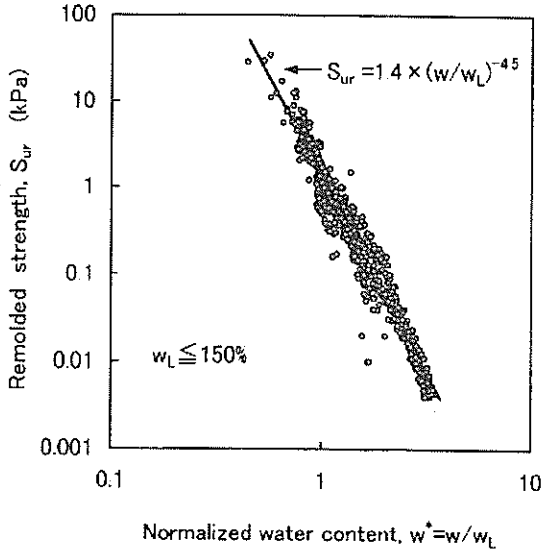

Figure 36(b) Relationship between shear strength of remolded clay and normalized water content

When the disturbed sample is consolidated one-dimensionally, the void ratio at each consolidation pressure becomes smaller than that of sample without the disturbance. The void ratio difference due to the disturbance is determined by the reconsolidation ratio R_{CR}, which is defined by the following equation;

$$R_{CR} = \frac{\ln (p/p_A)}{\ln R} \qquad (24)$$

where, p is the consolidation pressure and p_A is the initial effective stress after sample is disturbed and the consolidation starts.

As shown in **Figure 35**, the difference of specific volume f from the USC at the same consolidation stress is gradually reduced with increase of consolidation pressure accompanied with R_{CR}. Here the reduction ratio of specific volume r_f, is defined as follows;

$$r_f = \Delta(\ln f) \,/\, \Delta(\ln f)_0 \qquad (25)$$

where, $\Delta(\ln f)$ is the difference of specific volume from USC at the same consolidation pressure, and $\Delta(\ln f)_0$ is the initial value when the consolidation starts(Point A in **Figure 35**). At the initial condition of Point A, r_f=1, and r_f = 0 when the e-log p curve finally reaches USC by increase of consolidation pressure.

Okumura (1974) and Shogaki and Kaneko(1994) reported the change of e-log p curves of marine clays due to the degree of disturbance. Using the experimental data presented by Okumura and Shogaki et al, the relation between r_f and the reconsolidation ratio R_{CR} is plotted in **Figure 37,** where the relationship can be successfully expressed by the following equation;

$$\left.\begin{aligned} r_f &= 0.16(R_{CR} - 2.5)^2 \quad (R_{CR} \leqq 2.5) \\ r_f &= 0 \qquad\qquad\quad (R_{CR} > 2.5) \end{aligned}\right\} \qquad (26)$$

Eq.(26) means that, when the sample is remolded at an initial void ratio and then is reconsolidated, the e-log p curve returns to the USC when R_{CR} is larger than 2.5, i.e. the consolidation pressure is larger than $R^{2.5} \cdot p_B$. Using Eqs.(17),(23),(24),(25) and (26), the Standard Compression Curve from an initial void ratio SCC(e_0), can be written as follows:

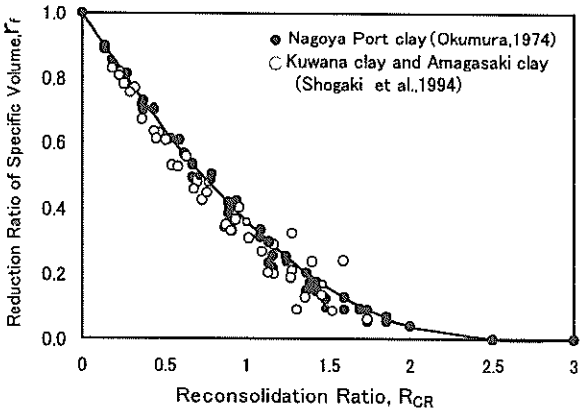

Figure 37 Reduction Ratio of Specific Volume, r_f, and Reconsolidation Ratio, RCR

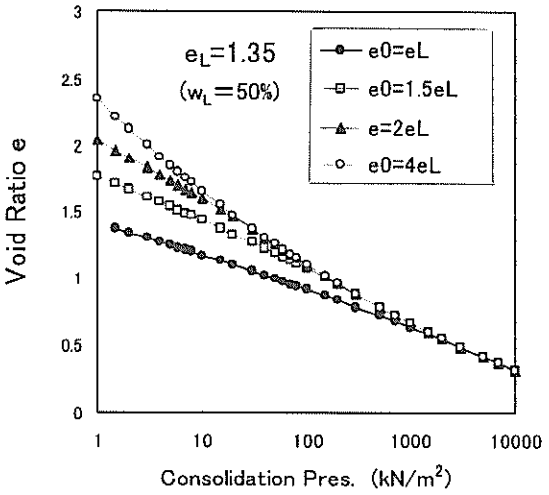

Figure 38(a) Calculated e-log p curves for different initial void ratios (e_L= 1.35)

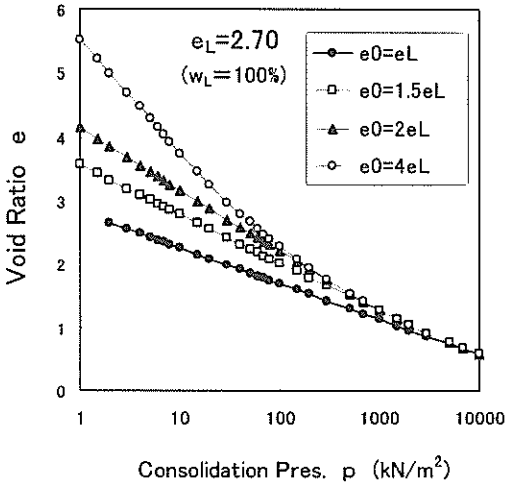

Figure 38(b) Calculated e-log p curves for different initial void ratios (e_L=2.70)

$$
\left.\begin{aligned}
&\text{when } p \leqq R^{2.5} p^* \\
&\quad I_{sv} = 1.47 - 0.27 \log p \\
&\qquad - 0.0186(\ln R)\{\ln(p/p^*)/(\ln R) - 2.5\}^2 \\
&\text{when } p > R^{2.5} p^* \\
&\quad I_{sv} = 1.47 - 0.27 \log p \\
&\text{where, } I_{sv0} = \ln f_0 / \ln f_L \ , \\
&\qquad p^* = 1.4 (e_0/e_L)^{-4.5} / (s_u/p)_{REM} \\
&\qquad R = 10^{(5.44 - 3.7 I_{sv0})} / p^*
\end{aligned}\right\} \quad (27)
$$

Comparing Eq.(27) with Eq.(17), the effect of the initial void ratio of consolidation, e_0 is given as $-0.0186 \ln R\{\ln(p/p^*)/\ln R - 2.5\}^2$, which is the difference from USC.

Figure 38(a) and (b) show the calculated standard compression curves of different initial void ratios as $e_0 = 1.0e_L$, $1.5e_L$, $2.0e_L$ and $4.0e_L$ (e_L is void ratio at liquid limit) for the conditions of typical Japanese marine clays as $(s_u/p)_{REM} = 1.0$, $w_L = 50\%$ ($e_L = 1.35$) or $w_L = 100\%$ ($e_L = 2.70$). As shown in figures, the f-log p curves calculated by Eq.(27) agree fairly well with the experiments for the various initial void ratios.

Imai(1978) examined the sedimentation and consolidation behaviors of fluid mud under gravitational force by a series of laboratory tests with sedimentation tubes. In his study, e-log p curves of remolded marine clays, whose initial water content were from 4 to 20 times larger than the liquid limits, were shown. In **Figure 39(a),(b),(c)** and **(d)**, Imai's experiments are re-produced on I_{sv} - log p relationship and the USC of Eq.(17) is shown for the comparison. As shown in **Figure 39**, the I_{sv}-log p relationship of 4 clays are not depending on the initial water content, and are very close to the USC.

Umehara and Zen (1982) carried out both the sedimentation tube test and the constant rate of strain (CRS) test to determine e-log p relationship of remolded marine clays for the large range of consolidation pressure. In **Figure 40,** the e-log p curves obtained by Umehara and Zen were plotted on I_{sv}-log p relation and compared with the calculated SCC($e_0=e_L$), SCC($e_0=1.5e_L$) and SCC($e_0=2e_L$). Although some scatters are seen, I_{sv}-log p relation is close to

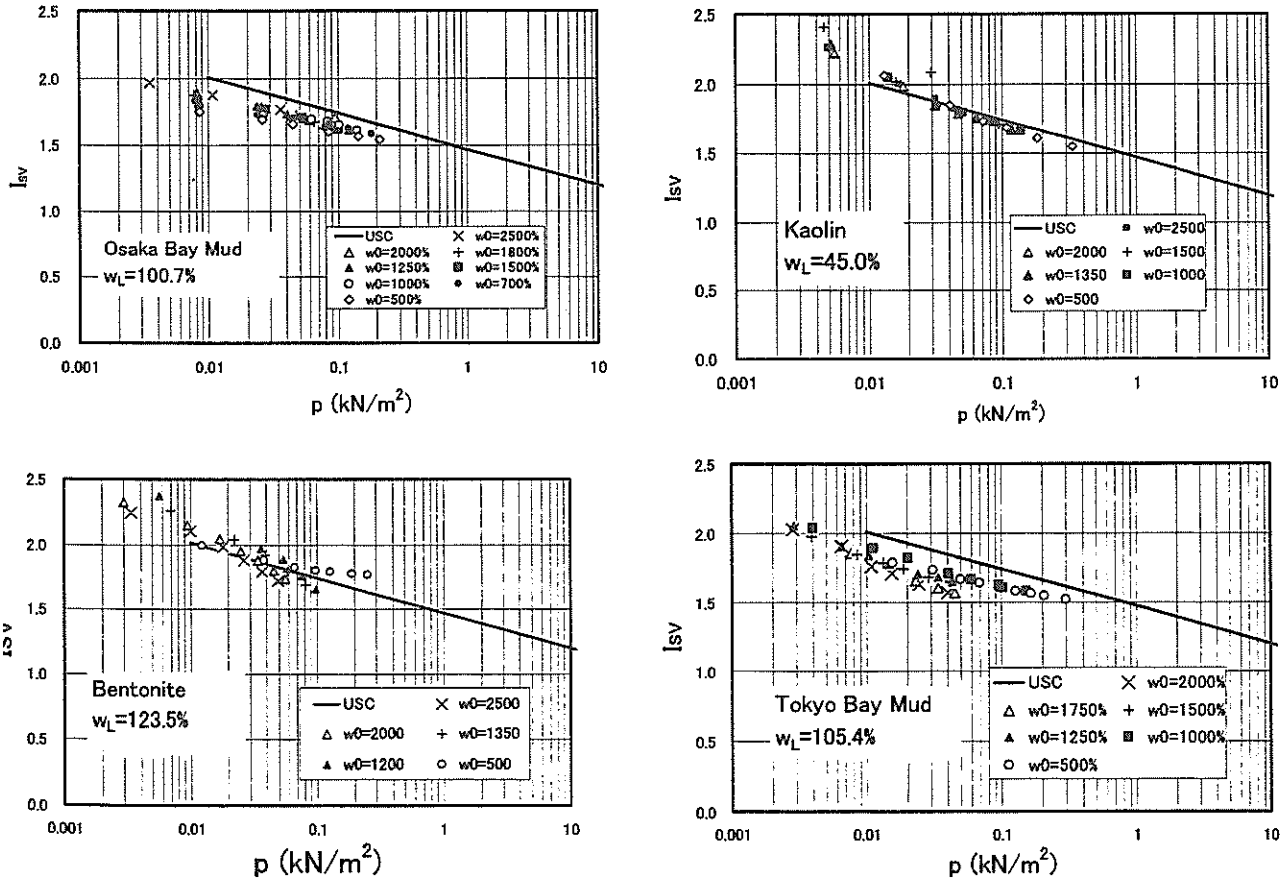

Figure 39 I_{sv}-log p curve of marine clays (data from Imai,1978)

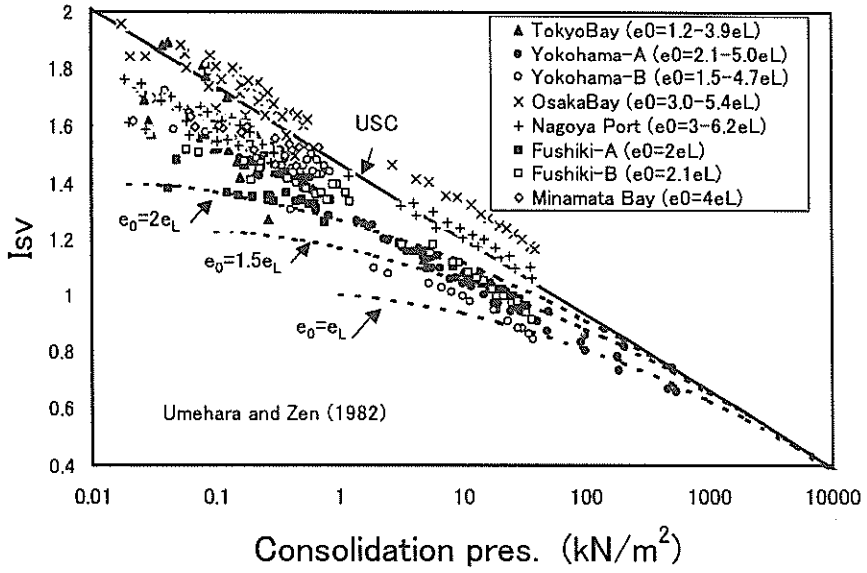

Figure 40 I_{sv}-log p relationship of reconstituted clays (data from Umehara and Zen, 1982)

USC when e_0 is large, and I_{sv}-log p relations shift to SCC(e_0) when e_0 becomes smaller. It can be concluded that the USC and SCC(e_0) obtained Eq.(27) is explaining various e-log p curves of remolded marine clays fairly well.

3.5 Initial void ratio of marine clay and normalized SCC for marine deposit

Holocene marine deposits are normally consolidated fine-grained soils that have been transported by river or tidal current and sedimented for recent thousands of years. Accordingly, by using the concept of standard compression curves, we can obtain the void ratio - effective overburden stress relationship, if an initial void ratio at the start of consolidation is known. It is considered that, even after the sedimentation, the soils with very high water content will behave like fluid, and will be moved very easily by the currents and waves. With decreasing the water content, they will settle down at some location and the consolidation will start at this moment.

Gomyo et al. (1986) studied the interaction between wave and bottom mud layer by the waterway experiment. The wave actions made the erosion and the movements of mud layer; at the same time, the wave height was reduced by the loss of the energy due to the interaction. The relationship between the damping ratio of wave height and the water content of mud layer is shown in **Figure 41**, where H and h is wave height and water depth, respectively, and bentonite (w_L=160%) and kaolin (w_L=48%) were used as the bottom mud. As shown in the figure, the interaction between wave and mud showed a peak at a specific water content, which were about 250% for bentonite and about 90% for Kaolin, regardless of the relative wave height H/h.

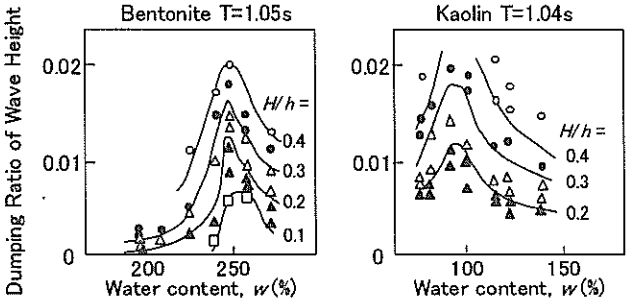

Figure 41 Damping of wave height and water content of bottom mud (Gomyo et al., 1985)

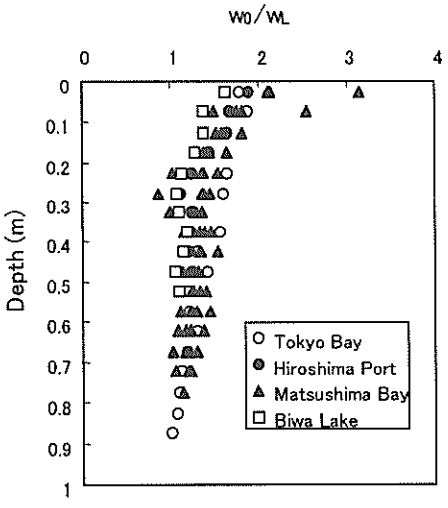

Figure 42 Normalized Water Content of Seabed (Depth = 0 — 1m)

This phenomenon can be explained as follows; when the water content is small, the mud layer has enough strength to be considered as rigid bottom, making no significant interaction, while, when the water content is large, the mud behaves like a fluid and moves with the same phase of water, making minor interactions. Accordingly, the largest interaction will take place, when the water content condition becomes a certain boundary value. As shown in **Figure 42,** the water content when the interaction showed the maximum were 1.5-2.0 times liquid limit of mud, which seems to be the boundary for mud between solid and fluid.

Inoue et al. (1990) also pointed out that the shear strength of remolded slurry increased remarkably when the water content becomes less than $2w_L$. This seems to agree with the results of **Figure 41**.

In **Figure 42**, the normalized natural water content w_0/w_L of sea floor at Tokyo Bay, Hiroshima Bay, Matsushima Bay, and Biwa Lake are shown with the depth. Most of marine clays near the sea floor have the water contents of 1.5 to 2.0 times the liquid limits. It can be assumed that the initial void ratios e_0 at the very beginning of consolidation of seabed is considered to be $1.5\text{-}2.0e_L$.

Based on these findings, the void ratio e_0 at the start of the consolidation of seabed is considered to be 1.5-2.0 times of the water content. **Figure 43(a)** and **(b)** showed the normalized water content, w_n/w_L, with the depth calculated by Eq.(27) under the conditions that $w_0 = 1.5w_L$, $w_0 = 2.0\ w_L$, w_L= 50-150%, and $(s_u/p)_{REM} = 1$. **Figure 43(a)** indicates that the calculated w_0/w_L at the sea floor agrees well with the field data in **Figure 42.** However, in **Figure 43(b)**, most of w_n/w_L values in the field are larger than the calculated, when the depth is more than 10m. The reason of this difference seems to be that the structure is formed by the aging effect in the field.

Assuming that the initial void ratios e_0 at the beginning of consolidation of seabed is 1.5 e_L or $2.0e_L$, standard compression curves SCC(e_0=1.5e_L) and SCC(e_0=2e_L) are calculated for the cases of e_L=1.0, e_L=2.0 and e_L=3.0. **Figure 44** shows the I_{sv} -log p relationships of SCC(e_0=1.5e_L) and SCC(e_0=2e_L).

As shown in **Figure 44**, I_{sv}-log p relationships of SCC (e_0=1.5e_0) and SCC(e_0=2e_L) are different depending on the liquid limit of soil. However, when accepting ±0.1 difference of I_{sv}, the difference is not so large, the average I_{sv}-log p curve can be determined for SCC(e_0=1.5e_0) and SCC(e_0=2e_L), respectively. The vales of I_{sv} of SCC(e_0=1.5e_0) and SCC(e_0=2e_L) are listed for consolidation pressures in **Table 2**, where the mean of I_{sv} is also calculated. Here the author calls the relation between the mean I_{sv} value and the consolidation pressure "standard compression curve for marine clay (SCC-marine)". SCC-marine is the standard e-log p relationship, when the ma-

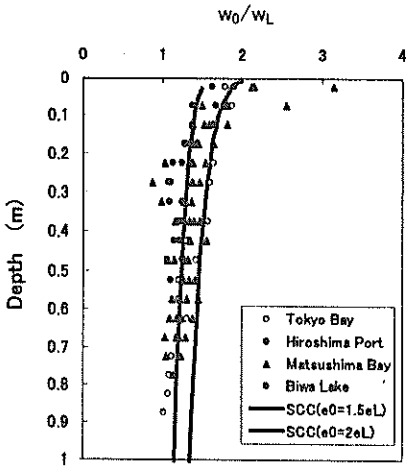

Figure 43(a) Calculated and field water content (Depth = 0 - 1m)

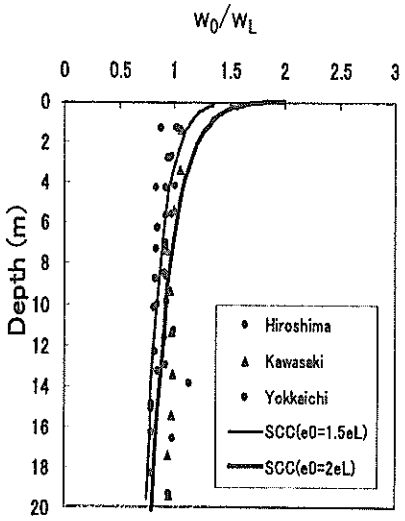

Figure 43(b) Calculated and field water content (Depth is 1 - 20m)

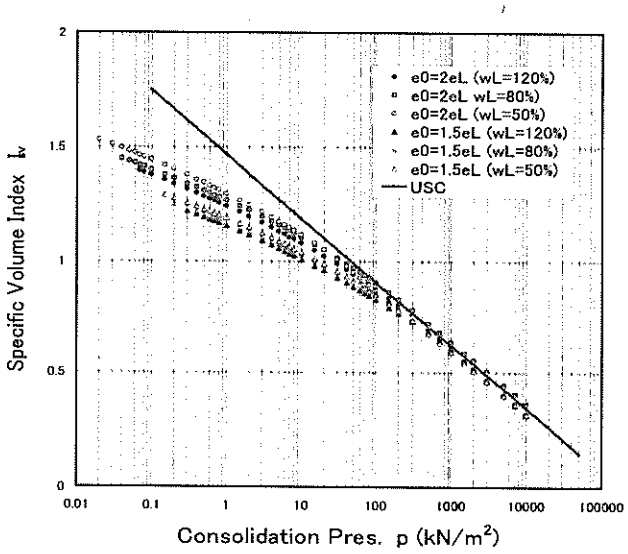

Figure 44 I_{sv} - log p relation of marine clay

rine deposits have been normally consolidated from the initial void ratio of 1.5-2.0e_L and not having any structure due to the aging. Accordingly, when the initial void ratio of marine clay is larger than that of SCC-marine at a consolidation pressure, the clay has a structure due to the cementation, while the void ratio is smaller than that of SCC-marine, the clay experiences a secondary compression or may be disturbed during sampling.

3.6 Intrinsic compression line and Sedimentation compression line by Burland(1990)

As a method to evaluate the structure of clay, Burland (1990) proposed a concept of intrinsic properties of clay. Burland showed that, most of the e-log p relationships of remolded clays, whose initial water contents are ranging from 1.0w_L to 1.5w_L, could be normalized into a unique I_v-log p curve by using the void index, I_v, defined as follows;

$$I_v = (e - e_{100}^*) / (e_{100}^* - e_{1000}^*) = (e - e_{100}^*) / C_c^* \quad (28)$$

where e_{100}^* and e_{1000}^* are void ratios when consolidation pressure are 100kPa and 1000 kPa, respectively. Further, the following equations to determine 2 parameters, C_c^* (= $e_{100}^* - e_{1000}^*$) and e_{100}^*, from the void ratio at liquid limit e_L , are given as follows;

$$C_c^* = 0.256\, e_L - 0.04 \quad (29)$$

$$e_{100}^* = 0.109 + 0.679 e_L - 0.089 e_L^2 + 0.016 e_L^3 \quad (30)$$

Burland called this unique I_v - log p relationship as the intrinsic compression line (ICL), and considered that ICL is inherent to the clay and independent of its natural state, that is, ICL shows the *standard* compression curve when clay have no structure due to aging.

When the void index I_v of normally-consolidated natural deposits is calculate with Eqs.(28)-(30) and plotted with the in-situ effective overburden stress σ_0' , there exists another unique $I_v - \sigma_0'$ relationship, which is called sedimentation consolidation line (SCL). **Figure 45** shows the ICL and SCL and the range of variation presented by Burland (1990). According to Burland, natural deposits on SCL have structures due to the aging effects of cementation or bonding, which constitute larger void ratios against the same effective overburden pressure.

In this study, the concept of ultimate standard compression curve, USC is proposed. All e-log p curves finally converge into USC, which is independent of structure due to the aging, initial void ratio and sample disturbance. When the initial void ratio e_0 is given, the standard compression curve, SCC(e_0) can be calculated by Eq.(27). In this sense, the USC and SCC(e_0) are *intrinsic* properties of clay.

A question on ICL concept of Burland is why the initial void ratio have to be 1.0e_L − 1.5e_L for ICL. Various e-log p curves of remolded clay can be easily produced in the laboratory when the initial void ratios are different. As discussed above, the initial void ratios of natural seabed are considered to be 1.5 − 2.0 times of e_L, while the initial void ratio of 1.0 − 1.5 times of e_L in ICL seems not to have any specific meanings. In the author's opinion, ICL is one of the SCC(e_0), whose initial void ratio is 1.0 w_L − 1.5 w_L . Although ICL concept may be useful for the reference of consolidation test of reconstituted clay, it does not have an

Table 2 I_{sv} on Standard Compression

Overburden stress (kN/m^2)	I_{sv} on Standard Compression Curve SCC(e_0=1.5e_L)	SCC(e_0=2e_L)	SCC-marine
1	1.17	1.27	1.22
2	1.13	1.22	1.17
5	1.07	1.15	1.11
10	1.02	1.10	1.06
20	0.97	1.04	1.01
50	0.90	0.95	0.93
100	0.87	0.92	0.90
200	0.78	0.81	0.79
500	0.69	0.70	0.69
1000	0.61	0.61	0.61
2000	0.53	0.53	0.53

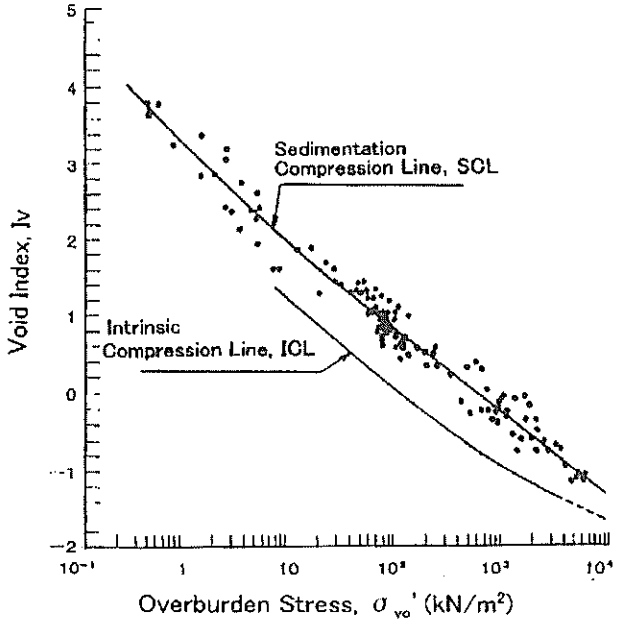

Figure 45 ICL and SCL proposed by Burland

intrinsic meaning on clay property.

Considering that the initial water content of seabed is approximately $1.5w_L - 2.0w_L$, the standard compression curves were calculated by Eq.(27) for w_L =70% − 110% with assuming that w_0 =1.75w_L . The average I_v - log p relationship of the calculated curves are named standard compression curve for marine deposits SCC-marine and plotted in **Figure 46**. As shown in **Figure 46,** void index I_v of *SCC-marine* is much larger than that of ICL and slightly smaller than that of SCL. This means that most of the difference between ICL and SCL can be explained by the difference of the initial void ratio of consolidation. The effect of the structure will be shown as the difference in I_v between SCL and SC-Marine, not between SCL and ICL.

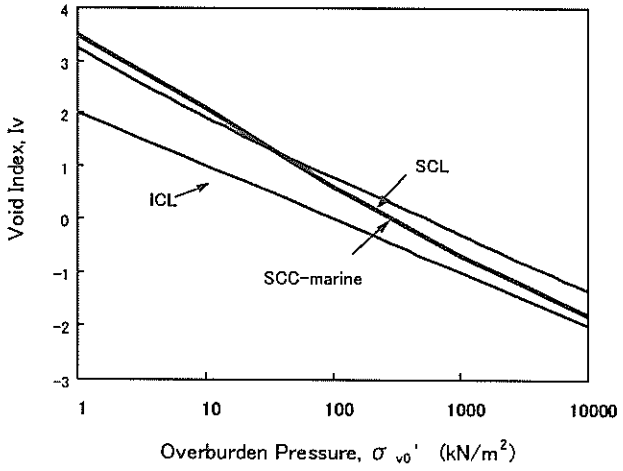

Figure 46 ICL , SCL and SCC-marine

3.7 Evaluation of structure based on I_{sv}-overburden stress relationship

The average I_{sv} − log p line of SCC(e_0=1.5e_L) and SCC(e_0=2.0e_L) is named SCC-marine. When in-situ void ratio e_0 is larger than the value given by USC, it is considered that the clay has a structure due to aging. Using the SCC-marine with the in-situ value of I_{sv}, the effect of structure can be evaluated quantitatively. When the difference ΔI_{sv} is obtained as shown in **Figure 47,** ΔI_{sv} is written as follows;

$$\Delta I_{sv0} = \frac{\Delta(\ln f)}{\ln f_L} = \frac{\ln f_0 - \ln f_{scc}}{\ln f_L} = \frac{\ln(V_0/V_{SCC})}{\ln f_L} \qquad (31)$$

where, f_0 is in-situ specific volume, and f_{SCC} and V_{SCC} are specific volume and volume of soil when the soil is on SCC-marine at the overburden stress, respectively. Eq.(31) can be written as;

$$\varepsilon_v = \ln(V_0/V_{SCC}) = (\Delta I_{sv0})(\ln f_L) \qquad (32)$$

where ε_v is expansive volumetric strain to the volume of soil on SCC-marine.

Using Eq.(32), the degree of structure can be indicated by volumetric strain. In the case that ΔI_{sv0}= 0.1 and f_L=3 (w_L=74%), ε_v = 0.1×ln 3 = 0.11, which means that the volume of clay is 11% larger than that without the structure. This clay layer potentially has a large compressibility, because the structure may be destroyed accompanied with consolidation due to the loading.

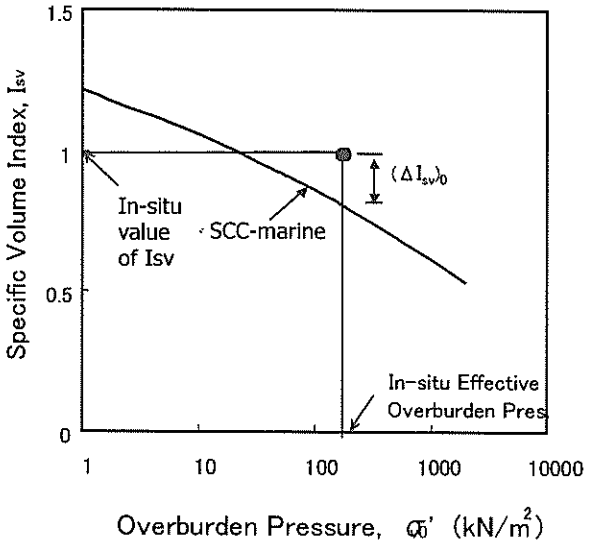

Figure 47 Difference of specific volume ratio, ΔI_{sv}

a) Holocene seabed

Figure 48 is the relationship between the specific volume ratio I_{sv} and the in-situ effective overburden stress σ_{v0}' at Holocene seabed in Tokyo Bay, Hiroshima Bay, Biwa Lake and Matsushima Bay, the largest depth of which is 20m. The average lines of standard compression curves SCC(e_0=1.5e_L) and SCC(e_0=2.0e_L) in **Figure 44** are indicated for the comparison. As shown in **Figure 48**, the I_{sv}-log σ_{v0}' relationship of natural seabed are plotted around the two SCC(e_0) lines, when p<40kPa. When p>40kPa, some soils show larger void ratios than those determined by SCC(e_0). This means that the void ratios of Holocene seabed in the shallow depth can be explained mainly by the compression characteristics of clay and the self-weight consolidation, and that no significant effect on the void ratio were seen by the aging.

b) Data collected by Skempton (1970)

The first study on the in-situ void ratio - overburden stress of normally consolidated deposits was presented by Skempton (1970). **Figure 49** shows reproduced I_{sv}-log σ_{v0}' relationship of 21 sites collected by Skempton. As shown in this figure, most of data are plotted around SCC(e_0=1.5e_L), and some are plotted along SCC(e_0=e_L). In the region of p> 400kPa, the values of in-situ specific volume index are larger than SCC and USC, suggesting that the cementation in the sedimentation process had formed structure and kept the void ratios larger. According to Skempton, when the sedimentation of clay starts at the tidal land, the initial water content become smaller than the case of sedimentation at the sea floor. Although the further study is necessary, this may be a reason of small in-situ void ratio along SCC(e_0=e_L).

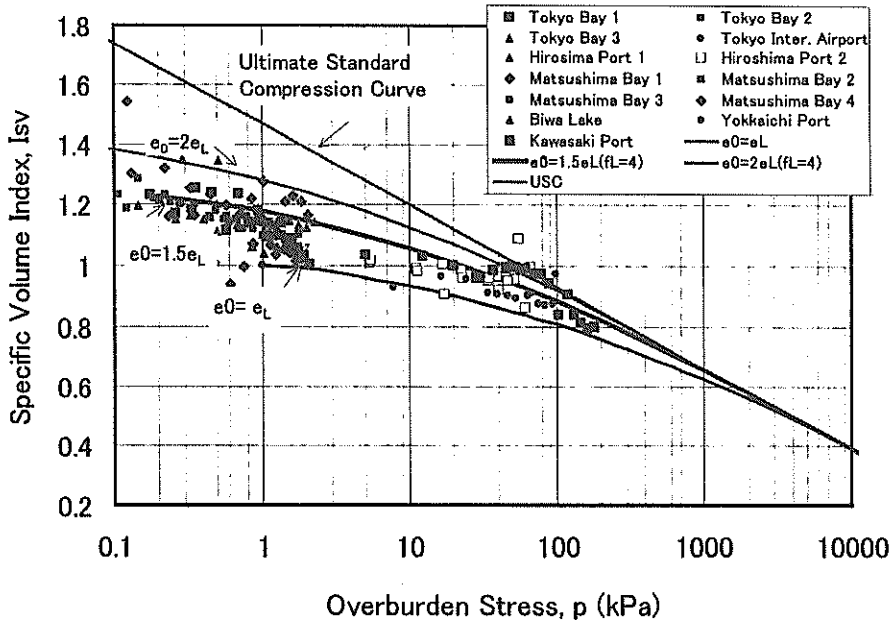

Figure 48 I_{sv0} — σ_{v0}' relationship (Holocene clay)

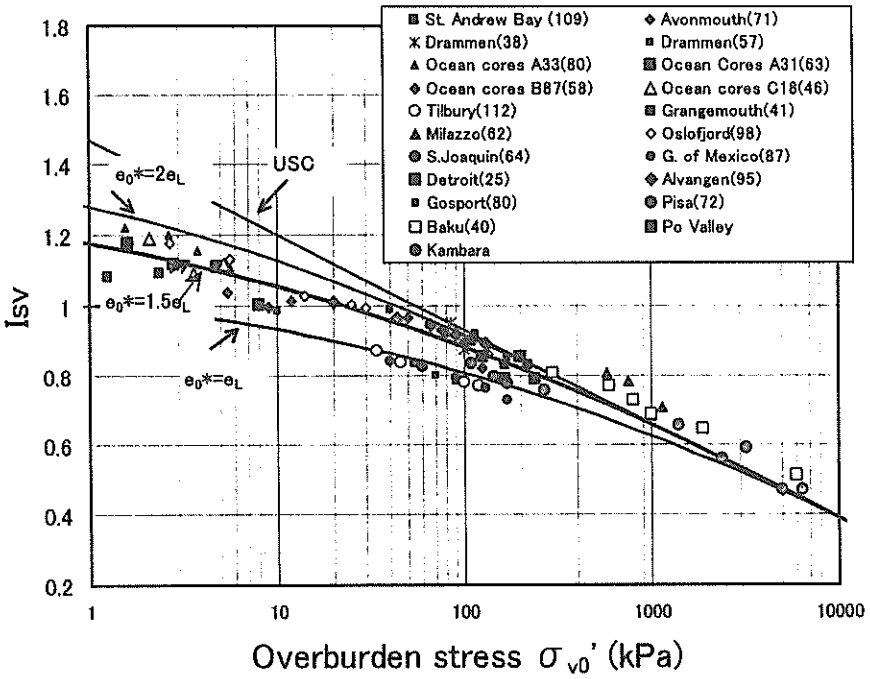

Figure 49 I_{sv0} — σ_{v0}' relationship of natural deposits (data from Skempton,1970)

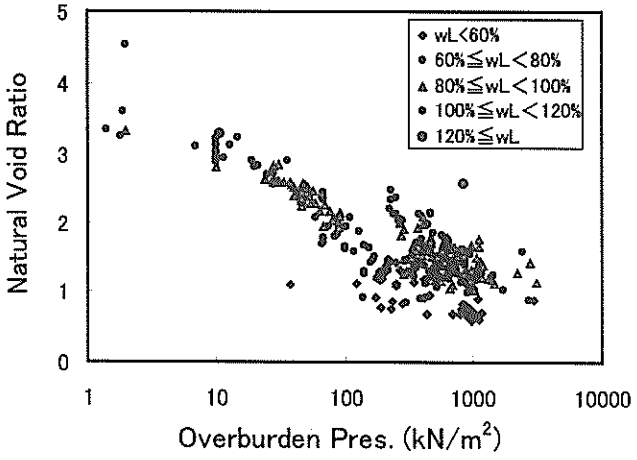

Figure 50 Relationship between void ratio and σ_{v0}' (Osaka Bay Pleistocene clay)

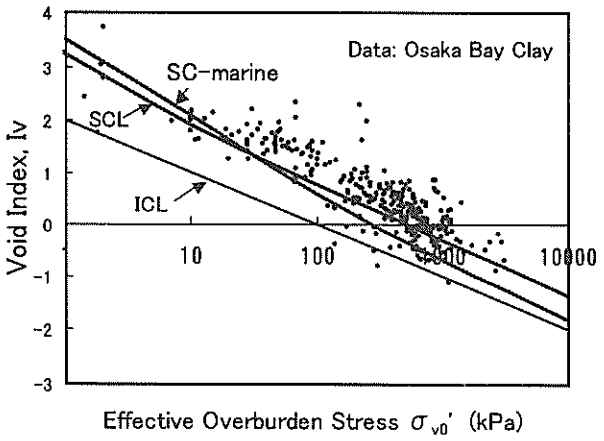

Figure 51 I_v - σ_{v0}' relationship of Osaka Bay Pleistocene clay

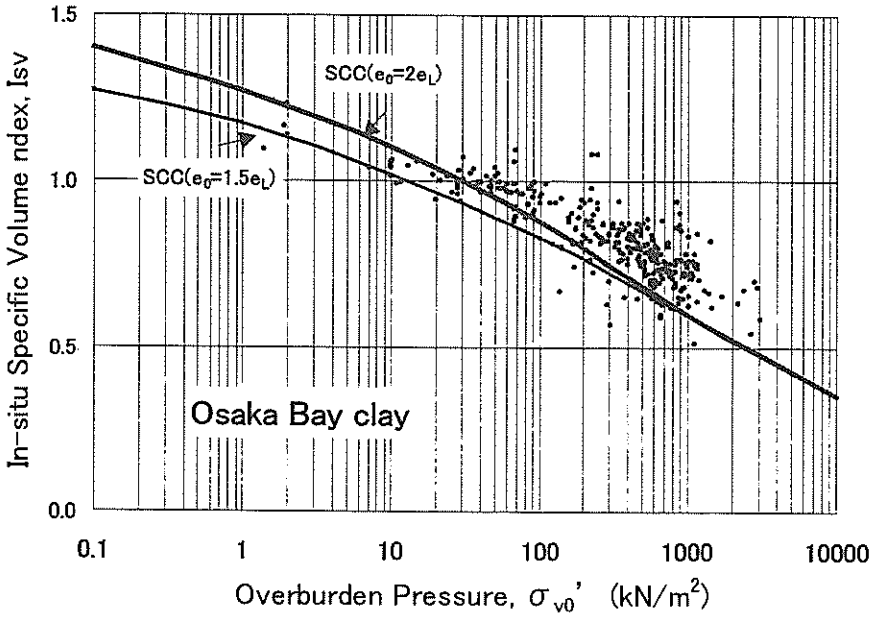

Figure 52 I_{sv0} — σ_{v0}' relationship of Osaka Bay Pleistocene clay

c) Osaka Bay Pleistocene Clay

As mentioned Chapter 3, undisturbed samplings and soil tests of clay up to 400m depths were carried out at the site in Osaka Bay, where the Holocene and Pleistocene deposits continue more than 400m, and the over-consolidation ratios of clay layers are ranging from 1.0 to 1.5 in all the depth (**Figure 4**).

Figure 50 is the relationship between the in-situ void ratio, e_0, and the overburden stress, σ_{v0}', at the site. As shown in **Figure 50** the void ratio decrease with the over-burden stress increase, depending on the liquid limit. The void index by Burland, I_v, is calculated by Eqs.(28)-(30), and plotted in **Figure 51**, where ICL, SCL and SCC-marine are also shown for comparison. As shown in **Figure 51**, the values of I_v in Osaka Bay Clay are much larger than SCL and SCC-marine.

The in-situ specific volume index I_{sv} and the effective overburden stress are plotted in **Figure 52**. As shown in **Figure 52**, the values of I_{sv} of Osaka Bay Pleistocene Clay are much larger than those determined by SCC(e_0=1.5e_L) or SCC(e_0=2.0e_L), which means that the clays in these area have larger void ratios or structures due to the cementation effects in the sedimentation process. Taking the mean of ΔI_{sv} in **Figure 52** as 0.15, and the mean water content of liquid limit w_L as 80%, expansive volumetric strain, ε_v, is

calculated by Eq.(32);

$$\varepsilon_v = 0.15 \ln (2.70 \times 0.8 + 1) = 0.17$$

This means that, due to the cementation effect during the sedimentation process, the volume of Osaka Pleistocene Clay layer are getting 17 % larger than those determined only by gravitational consolidation. **Figure 53** is typical e-log p curve of Osaka Bay Pleistocene Clay obtained by constant rate strain consolidation test. The extremely large compressibility is observed when the consolidation pressure gets larger than the consolidation yield stress p_c, which seems to be due to the destruction of the structure.

d) Ariake clay

Ariake clay is widely deposited around Ariake Bay in Kyusyu Island with an area of several hundreds of square km. Ariake clay is known as typical sensitive clay in Japan. Torrance and Otsubo (1995) reported that most of Ariake clays have sensitivity larger than 16, with the maximum over 1000. Ariake Bay Research Group (1965) has revealed that the upper Ariake layer above 11m was deposited under a marine condition, while the lower Ariake layer below 11m was deposited under brackish condition. The effect of salt extraction by leaching has been reported to be an important factor causing large sensitivity of Ariake clay (Torrance and Otsubo, 1995).

Figure 54 shows the in-situ I_{sv} — σ_{v0}' relationship of Ariake clays, which were taken from various sites around Ariake Bay, with the liquid limit w_L ranging from 51% to 164%. As shown in **Figure 54**, the values of I_{sv} of in-situ Ariake clay are extremely larger than those of SCC-marine. It is seen that the difference in I_{sv} from SCC-marine is more remarkable as the liquid limit of clay was smaller. The most probable explanation for this result is that Ariake clays sedimented under marine or brackish conditions with a high liquid limit. The leaching that occurred in the post-depositional process decreased the liquid limit, while the in-situ water content had little change. Accordingly, in the case of Ariake clay, the structure was not developed by cementation, but the SCC-marine was lowered by decrease of liquid limit due to leaching and consequently the value of I_{sv} increase drastically.

Figure 55 is an example of e-log p curve of Ariake clay sample, which was taken by high quality sampler and tested by constant rate strain consolidation test. Although the reason of high ΔI_{sv} value is different from Osaka Bay Pleistocene clay, the similar characteristics of structured clay, such as large compressibility at $p > p_c$ is clearly observed.

3.8 Summary

The concept of standard compression curve (e-log p

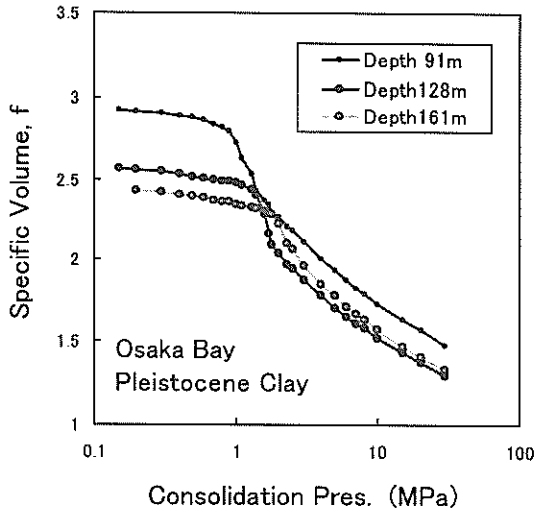

Figure 53 Typical e-log p curve of Osaka Bay

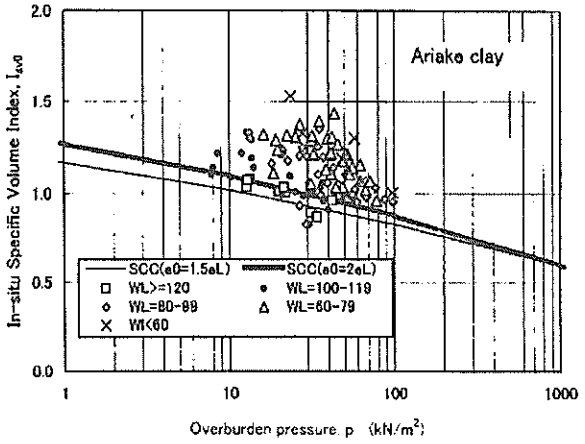

Figure 54 I_{sv0} — σ_{v0}' relationship of Ariake clay

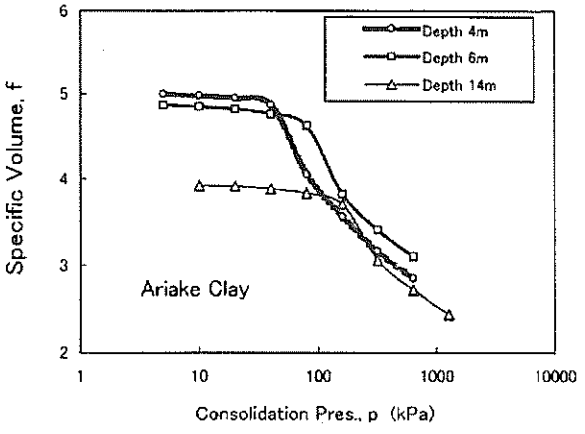

Figure 55 Typical e-log p curve of Ariake clay sample

curve) of clays was proposed. The standard compression curve consists of ultimate standard compression curve, USC, and the standard compression curves from an initial void ratio, SCC(e_0). USC is the e- log p relationship, where e-log p curves converge ultimately with increase of consolidation pressure. When the initial void ratio is small, the standard compression curve is different from USC. SCC(e_0) is the e-log p relationship that starts the consolidation at an initial void ratio e_0, and with the increase of the consolidation pressure, it finally converges into the USC.

Both curves are determined mainly by the liquid limit of clay and the void ratio at the beginning of consolidation. The uniqueness of USC was examined by the consolidation data of 18 marine clays. Using the specific volume index, I_{sv}, which is defined as ln (1+e) / ln (1+e_L), USC was shown as a unique I_{sv} – log p relationship not dependent on the plasticity of clays. I_{sv} – log p relationship of SCC(e_0) was also presented based on the USC concept and the study on sample disturbance by Okumura (1974).

It is considered that, under the conditions of marine waves and currents, the void ratio of marine clay at the beginning of consolidation is 1.5-2.0 times of liquid limit e_L. By calculating SCC(e_0) with the conditions of e_0=1.5e_L and e_0=2e_L, the standard relationship between I_{sv} and the effective overburden pressure, σ_{v0}', was obtained for normally consolidated marine deposits, which is called SCC-marine. By comparing the in-situ specific volume of clay with the value on of SCC-marine, the degree of structure of marine deposits can be evaluated and the followings findings were obtained:

1) The void ratios of Holocene seabed in the shallow depth can be explained mainly by SCC-marine and that no significant effect by aging on the void ratio.
2) As the in-situ values of I_{sv} of Osaka Bay Pleistocene clay at the site of Kansai International Airport are much larger than those of SCC-marine, the clays seems to have well-developed structure due to aging.
3) The values of I_{sv} of in-situ Ariake clay prefecture were extremely larger than those of SCC-marine. The cause of high I_{sv} value is considered to be the decrease of liquid limit by leaching that occurred in the post-depositional process.

4. CONSOLIDATION BEHAVIOR OF OSAKA BAY PLEISTOCENE CLAY

4.1 Separate-type consolidometer

Osaka Pleistocene clay shows a remarkable increase in compressibility when the overburden pressure exceeding the consolidation yield stress is loaded. It is usually revealed with a high consolidation yield stress which is believed to be originated not only by the high overburden pressure, but also by its well-developed structure resulting from long-term secondary compression and aging effects.

It is therefore necessary to adopt more elaborated and sophisticated method for the investigation on this type of clay retaining peculiar compressibility characteristics in the purpose of proper understanding on the development of deformation and pore water pressure.

A separated-type consolidometer test, in which the soil layer is divided into five inter-connected sub-specimens, is carried out for Osaka Pleistocene clay. Several researchers have conducted the separated-type consolidation test mostly in the purpose of verification of various consolidation theories (Berre and Iversen, 1972, Mesri and Choi, 1985, Aboshi et al., 1985, and Imai and Tang, 1992). However most of the soils used in their studies were artificial reconstituted soils or undisturbed Holocene clays with less developed soil structure. For the typical condition of Osaka Pleistocene clay with high consolidation yield stress and with its well-developed structure, a separated-type consolidometer of high capacity was specially designed. With this device, the some particular consolidation characteristics of undisturbed Osaka Pleistocene clay are to be investigated.

4.2 Method and procedure

The fundamental concept of separated-type consolidometer test is illustrated in **Figure 56.** The soil specimen is separated into several inter-connected samples, so that the consolidation characteristics of the soil by thickness variation together with the internal variation of pore water pressure can be examined in connected test

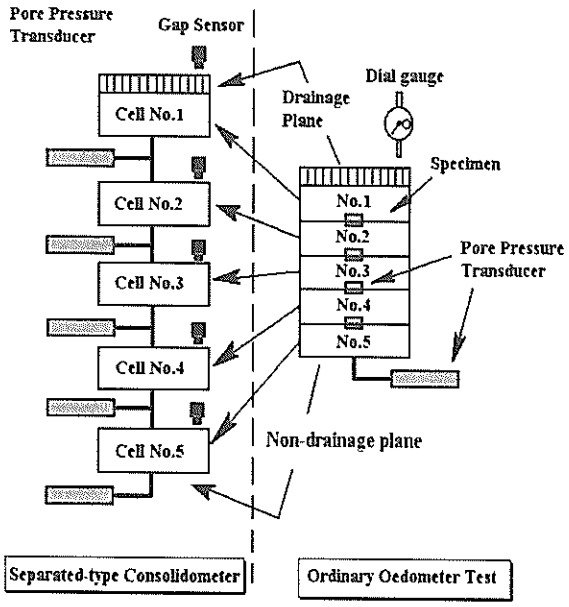

Figure 56 Concept of separated-type consolidation

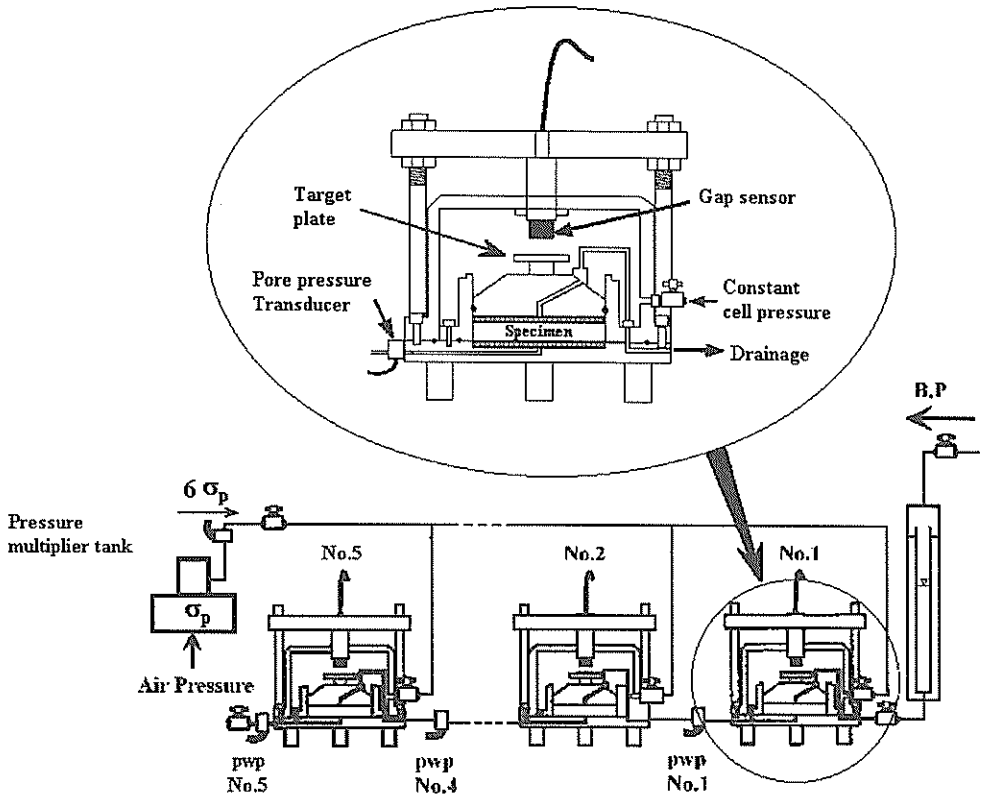

Figure 57 Systematic diagram of the separated-type Consolidometer

cells. Those are usually impossible to be obtained in the conventional type of oedometer test. The bottom drainage plane of one sub-specimen is connected to the top drainage of the next one in the series.

Figure 57 shows the systematic diagram for the separated-type consolidometer test. The cell is made of metallic body to endure the high pressure and the drainage between sub-specimens is also carried by copper pipes to support high pore water pressures during the tests. Pore water pressure is measured at the bottom of each sub-specimen by pressure transducers. To increase saturation of the specimen, backpressure is applied to the drainage surface of the top specimen.

A gap-sensor of non-contact type measuring the gap distance by magnetic pulse between the sensor and the target plate on the loading cap is employed. A soil sample trimmed into five sub-specimens, 60mm in diameter and 10mm in thickness each, was used for this test. Each sub-specimen was placed into the consolidometer cells, labeled No.1, No.2, ···, and No.5. This gives a total maximum length of 50mm for the whole drainage path. The drainage was allowed only at the upper boundary of sub-specimen No.1 cell and the drainage volume was measured for the total volume change by a burette in which back-pressure is applied.

Soil properties of Osaka Pleistocene clay used in this test are shown in **Table 3** Osaka Pleistocene clay tested in this study was collected from the soil layer of 150~170m depth below the sea water level. The specific volume index I_{sv} is 0.682 and the difference of I_{sv} from SCC-marine, ΔI_{sv} is 0.072, which means this layer is highly structured with the expansive volumetric strain of 9.9%. Recently, it has been known that a large amount of Diatom microfossils are contained in Osaka Pleistocene clay and they may a major influential factor for the large void ratio and the high compressibility (Tanaka and Locat, 1999).

To compare the effect of soil structure, reconstituted soils from the same Osaka Pleistocene clay were prepared for the comparison of test results. For the preparation of a re-

Table 3 Soil properties of Osaka Pleistocene clay

Natural water Content, w_n (%)	Liquid limit, (%)	Plastic limit, (%)	Specific gravity, G_s
53.8 - 57.8	73.6 - 108	31.1 - 36.6	2.69 - 2.72

constituted sample, the soil passed with 106μm sieve, was remolded and mixed thoroughly at the water content of above 180%, which is almost twice the liquid limit of soil to eliminate the possible effect of soil structure. Then it was pressurized in a cell up to 196kPa by step loading until the 95% of consolidation by $\sqrt{t}$ method was obtained. **Figure 58** shows the void ratio – effective stress curve obtained from the consolidation test by constant rate of strain (CRS) comparing the reconstituted and the undisturbed soil used in this test. The consolidation behavior of undisturbed Osaka Pleistocene clay can typically explained by some typical features like low compressibility in the over consolidated range, sudden decrease of void ratio after yielding and non linear relations for the void ratio with logarithm effective stress in the normally consolidated range (also refer to **Figure 32**).

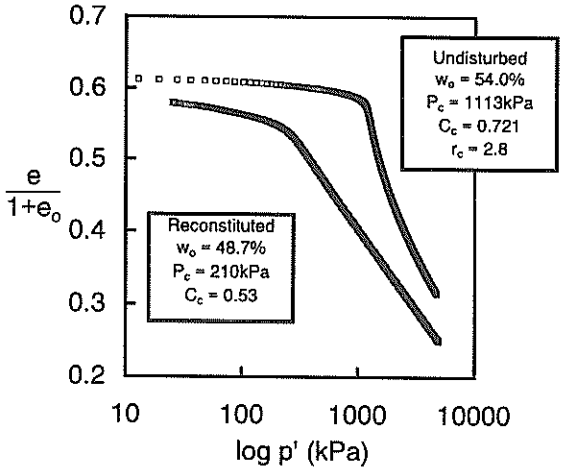

Figure 58 Comparison of e-log*p* for reconstituted and undisturbed Pleistocene clay

4.3 Test results and discussions

The pressure of each sub-specimen by the increment of loading are measured at a given measuring time. Back-pressures were applied by 196kN/m^2 for reconstituted soil and by 392kN/m^2 for undisturbed soil. Five sub-specimens in series were used both for the reconstituted soil and disturbed soil.

Figures 59 and **60** show the variation of strain and excess pore water pressure as a function of time for each increment of stage loading for the reconstituted and the undisturbed sample respectively. In the case of the recon-

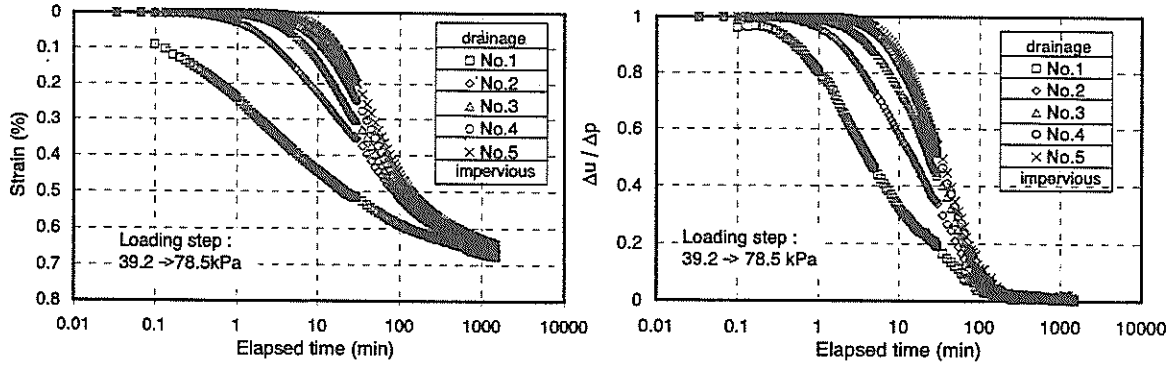

(a) Over-consolidated range

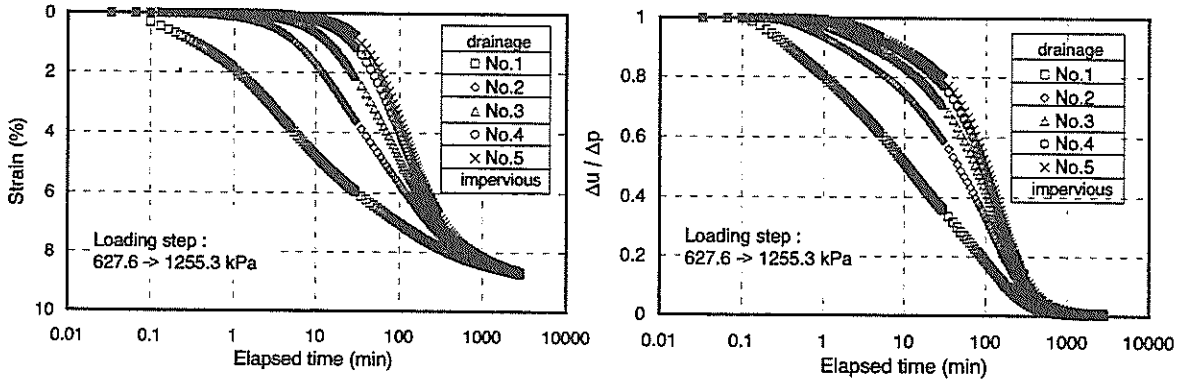

(b) Normally consolidated range

Figure 59 Variation of strain and pore water pressure with elapsed time (Reconstituted clay)

stituted sample, the delay of compression by the distance from the drainage surface was clearly seen in both over consolidated and normally consolidated range. This delay of compression is due to the fact that sub-specimen nearer to the free drainage boundary is compressed faster by taking place of rapid dissipation of excess pore water pressure.

Comparing over-consolidated compression with normally consolidated compression, no distinctive difference of the consolidation behavior was observed except an in-

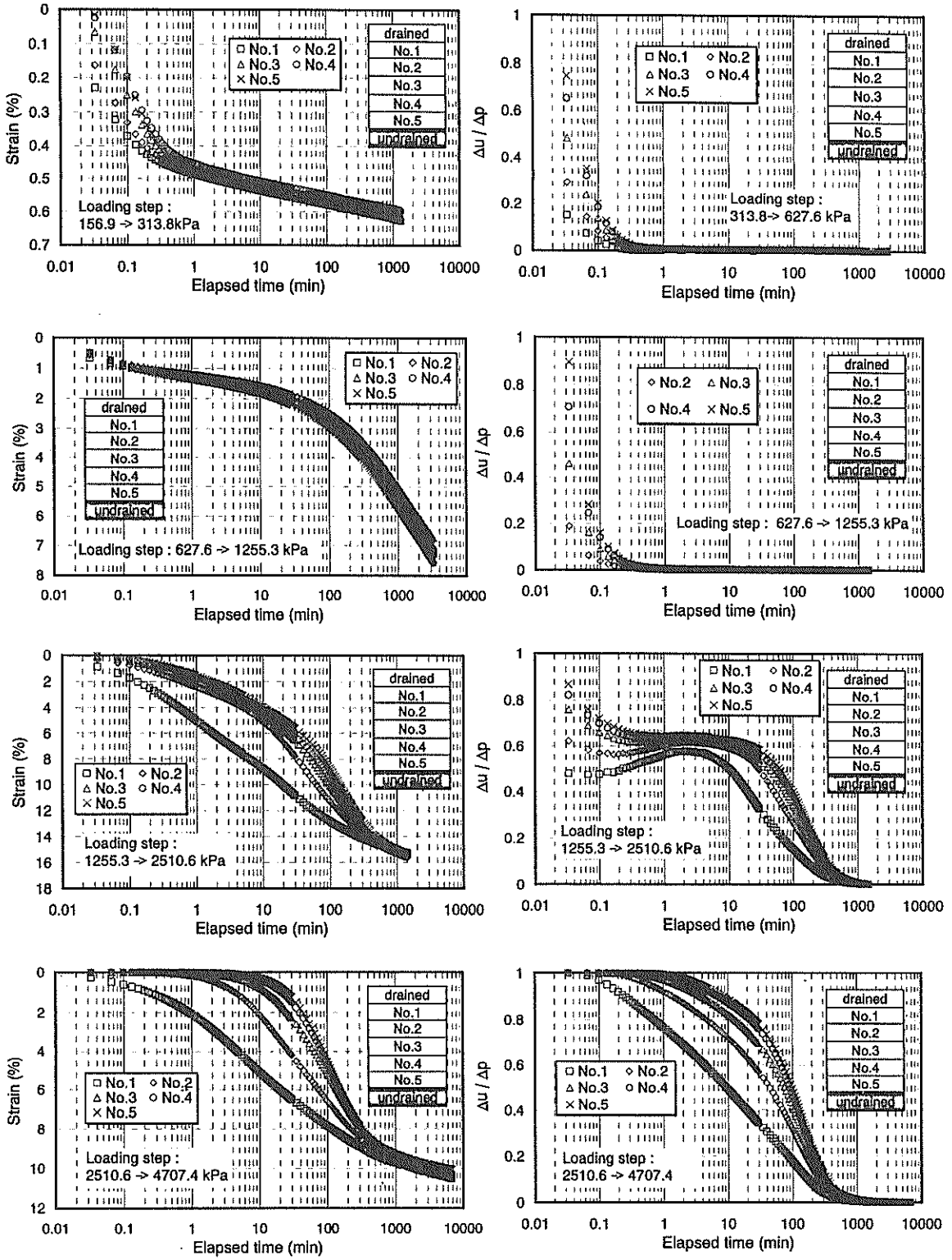

Figure 60 Variation of strain and pore water pressure with elapsed time(Undisturbed clay)

crease in primary strain and coefficient of secondary consolidation in the normally consolidated range.

However, for the undisturbed sample of Osaka Pleistocene clay, the consolidation behavior showed evident contrast between the normally consolidated and the over-consolidated ranges as it can be seen in **Figure 60.** In the over-consolidated range, primary consolidation is over almost instantly and all subsequent strains for all sub-specimens continue at nearly constant rate of secondary compression. Excess pore water pressure also showed instant dissipation within a minute, which means almost no excess pore water pressure was developed in the over consolidated region. It is not so difficult to understand the rigidity of the soil structure against overburden pressure.

Meanwhile it is interesting to say that the dissipation characteristics of excess pore water pressure at the loading stage exceeding the consolidation yielding stress of undisturbed soil, displayed very unique aspect. As the stage loading closes to the consolidation yielding stress, the compressibility of soil started to increase dramatically with little development of excess pore water pressure. However once the soil underwent yielding, the soil began to display the delay of compression according to the drainage length to the drainage surface.

Particularly it is distinguishable to see the peculiar development of excess pore water pressure at each sub-specimen. Once the variation of excess pore water pressure showed the decreasing tendency at first, then it increased again to a notable degree after the soil experienced yielding. For the main reason of this, it is considered that excess pore water pressure once barely developed in the over-consolidated range was affected by the rapid increase of compressibility progressing in the loading stage shifting over to the normally-consolidated range. This means that the rate of increase in compressibility became much higher than the rate of excess pore water pressure dissipation when skeletons of Osaka Pleistocene clay with well-developed structure were yielded by a high overburden pressure. However it is necessary to point out that this behavior is highly affected by the size of loading increment and consolidation yielding stress.

In the normally consolidated range, the consolidation behavior of soil showed delay of compression with distinct delay of dissipation of excess pore water pressure from the start of drainage. Those behaviors in normally consolidated range revealed almost similar variation characteristics to the results for reconstituted sample.

In **Figure 61**, the distribution of degree of consolidation, U_z to the thickness of soil layer according to the length of drainage path is compared with theoretical solution by Terzaghi's one-dimensional consolidation theory. Both soil conditions are for the loading spanning the preconsolidation pressure.

For the reconstituted sample, the distribution of U_z to the depth of soil from measured values is incidentally well consistent with theoretical solutions. Of course, this is always the same with different type of soils or different test conditions. At any rate, from the figures, it can be said that, even though the primary consolidation of undisturbed soil is once ended up at much higher rate than that of reconstituted one after yielding, the consolidation process became greatly delayed and showed complexity at the consolidation process.

Relations between void ratio and effective stress are shown respectively for reconstituted and undisturbed samples in **Figure 62**. For the comparison, void ratio is normalized with the initial void ratio, e_o. It is clear that the e-log p' relation from the results by separated-type consolidometer test is not linear either with any load increment or with the length of drainage path for both sample conditions. Due to the fact that, at the soil layer which is

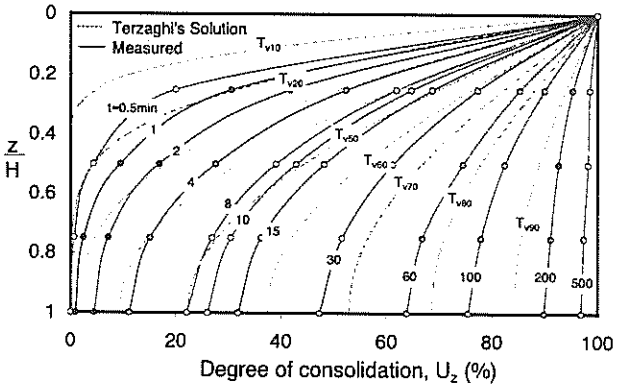

(a) Reconstituted soil

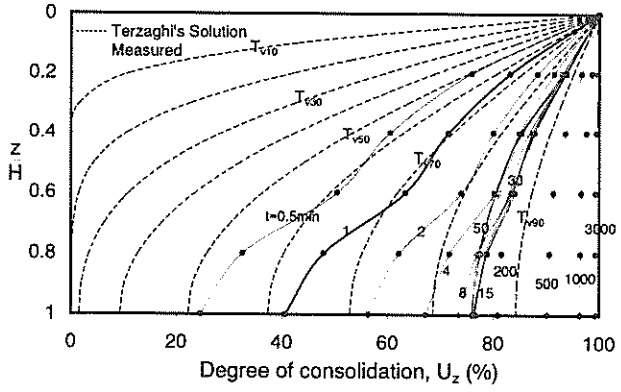

(b) Undisturbed soil

Figure 61 Degree of consolidation with depth of soil

near to the drainage boundary, effective stress instantaneously increased, the curve for No.1 layer reveals the e-log p' relation almost close to the ideal no water condition with the largest curvature. However it is notable that varied relation of e-log p' by the length of drainage path for undisturbed sample can be observed at the next load increment after exceeding the preconsolidation pressure.

And also for the undisturbed soil, before the substantial increase of compressibility after preconsolidation pressure, large span of over-consolidated range with respect to the increase of stress implies high resistance of soil structure. It is notable that sudden increase of compressibility can be observed near the consolidation yielding stress at almost constant effective stress for all sub-specimens following the same curvatures. After yielding, tremendous decrease of void ratio took place at subsequent loading pressures after yielding, revealed with almost two third of total decrease in void ratio.

4.4 Summary

Using separated-type consolidometer of high capacity designed in this study, the consolidation characteristics of Osaka Pleistocene clay was examined with the purpose of investigating soil structural effect. Through the tests as a fundamental stage, undisturbed soil in the over-consolidated range showed extremely faster expulsion of excess pore water pressure than the normally consolidated range and that the most part of consolidation settlement is occupied by secondary compression at a given pressure increment.

At the pressure increment spanning the preconsolidation pressure of Osaka Pleistocene clay, effective stress increasing with elapsed time showed sudden decreasing tendency after the effective stress exceeded the preconsolidation pressure. It is estimated that the cause of this unique behavior is to be attributed to the fact that radical increase of compressibility by the yielding of soil structure surpasses the dissipation rate of excess pore water pressure. This behavior is particularly relevant to clays with a well-developed structure such as Osaka Pleistocene clay.

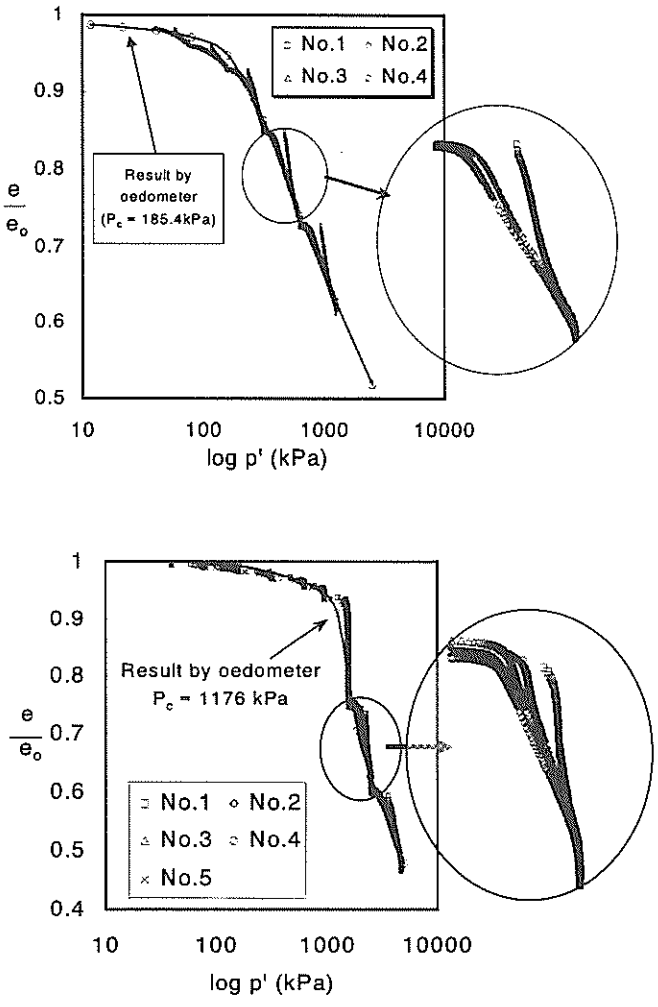

Figure 62 *e*-log *p* curve by separate type Consolidometer

5 STRENGTH OF OSAKA BAY PLEISTOCENE CLAY - CASE OF KIA PROJECT -

5.1 Importance of shear strength of Pleistocene Clays in KIA second phase project

In second-phase project in Kansai International Airport, the shear strength of Pleistocene clay layer at the large depth has become important design problem. In the first-phase project, the shear strength of Pleistocene clay was not studied in detail because the stability analysis of the seawall structures indicated that the safety factors against deep-seated slip circles passing through the Pleistocene clay layer were much greater than the required design safety factor of 1.3. However, as the water depth and the reclaimation become larger in the second-phase project, the slip circle that gives the minimum safety factor possibly passes through the Pleistocene clay layer.

Undisturbed samples used in this study were obtained from Osaka bay in 1995 during the in-situ investigation for second construction phase of the Kansai international airport. The location of boring are shown in **Figure 63(a)**. The borings carried out as deep as 400m indicated that the average depth of water was 19.2m and the depth of alluvial soft clay was 25m. The sampling method and the characteristics of soils collected from Osaka bay were reported in detail by Horie et al. (1984), Ishii et al. (1984) and Tsuchida et al. (1984).

Figure 63(b) shows the consistency profiles including liquid limit, w_L, plastic limit, w_P and natural water content, w_0. Although, only the clay and sand layers have been deposited alternately, only the clay layers were studied, because the shear strength data of the clay is significant for the stability analysis.

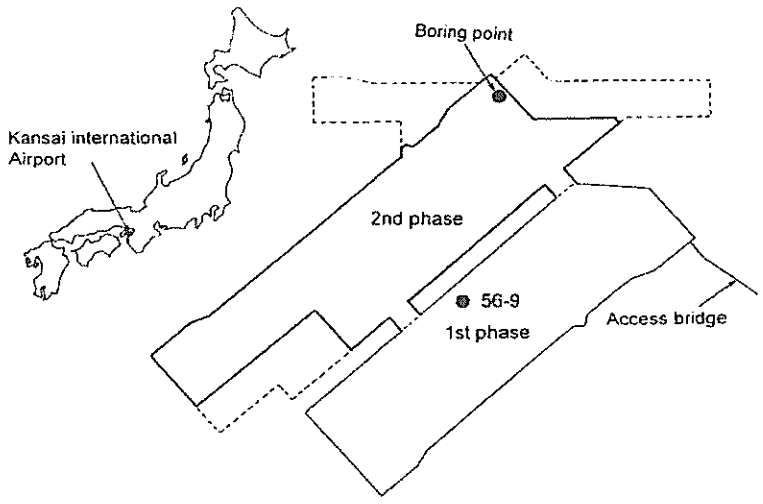

Figure 63(a) Location of undisturbed sampling

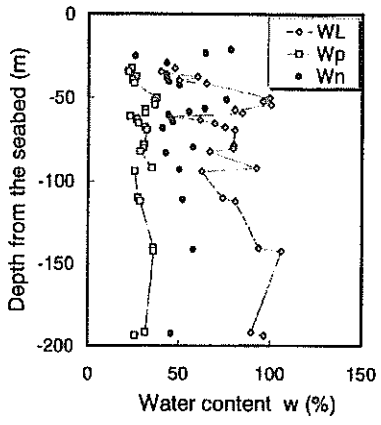

Figure 63(b) Consistency profile of Pleistocene clays

5.2 Measurement of residual effective stress of undisturbed sample

Evaluation of sample quality by measuring suction, which corresponds to residual effective stress of sample, was firstly attempt by Okumura (1974). Shimizu and Tabuchi (1993), Shogaki et al. (1995) and Mitachi and Kudo (1996) measured the residual effective stress of sample and corrected the unconfined compression strength. As most of these researches studied on saturated Holocene clays, the measured data of suction were less than vacuum (98.1kN/m^2). On the other hand, Mitachi and Kudo(1996) measured suction larger than 98.1kPa in Kaolin clay, applying a back air pressure.

To evaluate the quality of Pleistocene clay samples, the measurement of suction was carried out. The suction measuring system used in this study is schematically illustrated in **Figure 64**. The system can measure the suction, by placing the specimen under a certain high air pressure u_a (back air pressure). The specimen trimmed as 35 mm in diameter and 80mm in height is placed on the ceramic filter which has an air entry value of 200 kN/m^2 and is saturated by de-aired water previously. After setting the cell, air pressure was applied up to a certain value u_a, and the valve, which is placed between inside of ceramic filter and inside of cell, was opened for a moment to balance both pressures in the pedestal and in the cell.

Figure 65 shows an example of data sets measured by suction tests, which were conducted on specimens taken from the depth of 93m. The measured suction under atmospheric condition was approaching to the vacuum, however much smaller than the suction when the back air pressure was applied. When the back air pressure was larger than 100kN/m^2, the measured residual stresses became constant with not dependent on the back air pressure. The constant value of the suction is considered to be a true residual stress of the specimen.

Figure 66 shows the variation of residual effective

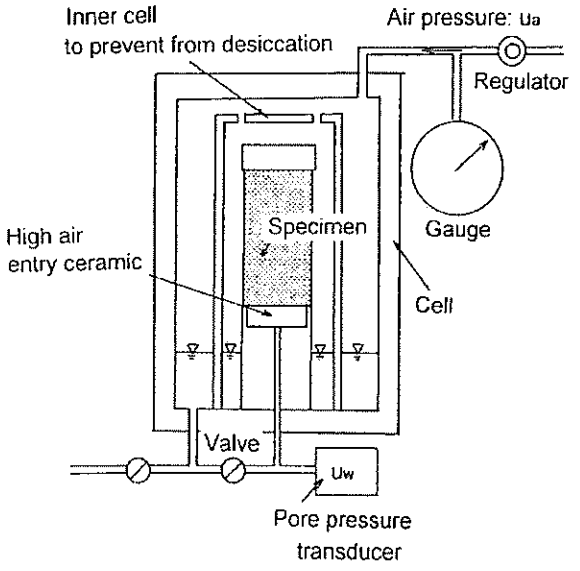

Figure 64 Measurement of suction under applying back air pressure

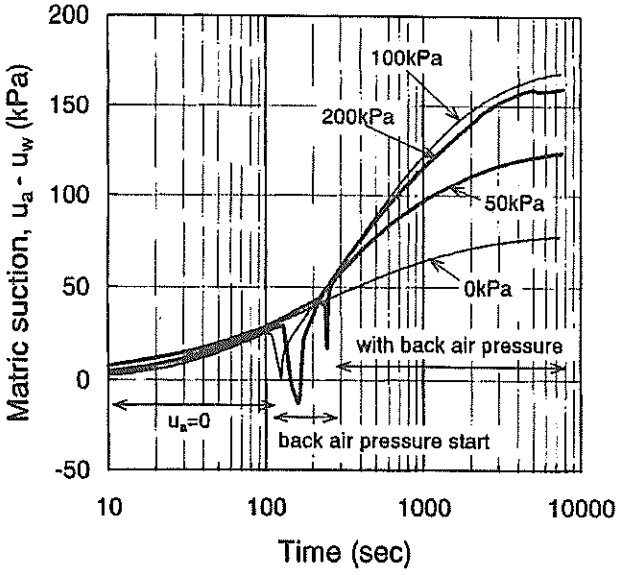

Figure 65 Measured suctions under different back air pressure

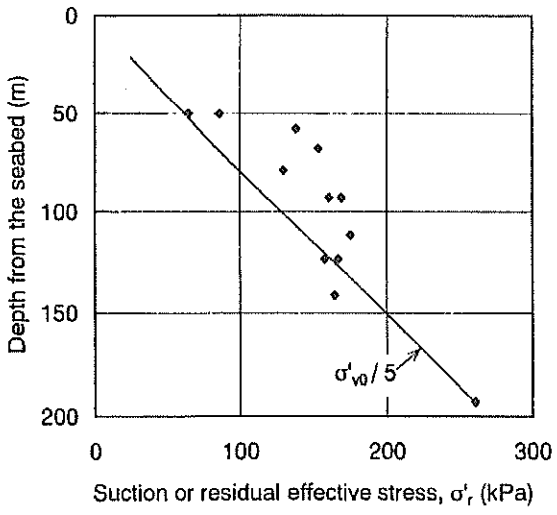

Figure 66 Residual effective stress of sample with depth

stresses based on the measured suction Osaka Bay Pleistocene clays taken from different depths. As shown in the figure, the residual effective stresses in Pleistocene clays collected from large depth were equal to or more than one fifth of effective overburden stresses. These values are consistent with the test results of Tanaka, M. et al. (1995), who reported that residual effective stresses of Japanese Holocene clays are between one forth and one sixth of effective overburden stress. According to Okumura (1974), when the residual effective stress is equal to or more than one fifth of effective overburden stress, the disturbance ratio *R*, an index of sample quality, ranges from 1.5 to 3, which means that the sample quality is classified to "very good". It can be said that quality of undisturbed samples of Osaka Bay Pleistocene clay are better than anticipated, although they were collected from large depths.

5.3 Recompression method

The recompression method is aimed to reduce the effect of disturbance, in which the shear test is conducted after the specimen is consolidated by the in-situ effective stress conditions in triaxial cell (Berre and Bjerrum, 1973). In this method, a specimen from undisturbed sample is first consolidated under K_0 condition at the same effective stresses in the field, and after the completion of consolidation, it is subjected to shear under undrained condition. Hanzawa and Kishida (1982) and Hanzawa (1982) applied the shear strength obtained by the recompression method for stability analyses of several practical projects and reported excellent agreements between the analyses and the field behaviors. In testing procedures of Hanzawa, K_0-consolidation was carried out by the end of primary consolidation, and the average shear strength of compression and extension loading at strain rate of 0.01%/min were used for considering the effects of strength anisotropy and time to failure.

In this study, the recompression method similar to the procedure by Hanzawa was used. It must be noted that, although the shear strain rate of 0.01 %/min is recommended, the rate of 0.1 %/min was adopted to complete a number of tests within a limited time, and no correction on the shear strain rate was carried out. K_0 value was first determined by K_0-consolidation test in the triaxial test (Tsuchida et al., 1989). For the recompression method, the in-situ stress conditions must be applied without destroying the structure as much as possible by K_0 consolidation. Anisotropic consolidation was carried out by increasing the stresses linearly until $\sigma'_1 = \sigma'_{v0}$ and $\sigma'_3 = K_0 \cdot \sigma'_{v0}$ in 720 min and this condition was maintained until the excess pore pressure was completely dissipated. After that, the specimen was sheared in undrained condition for compression (CAUC) or extension (CAUE) loading with the axial strain rate of 0.1%/min.

As a simplified procedure of recompression, Tsuchida et al. (1989) proposed the Simple CU (consolidated undrained) test for a practical purpose. The Simple CU test is a CIU (isotropically consolidated undrained) compression triaxial test, in which an isotropic consolidation under the mean in-situ effective confining stress of $(1+2K_0)/3 \cdot \sigma'_{v0}$ is carried out, instead of the K_0 consolidation. For the stain rate, 0.1 %/min is recommended. They also proposed to take 75 % of the shear strength measured from the simplified CU test as the design strength, to account for the strength anisotropy and time effect.

Both in Bjerrum's method and Hanzawa's method of recompression (Berre and Bjerrum, 1973; Hanzawa and

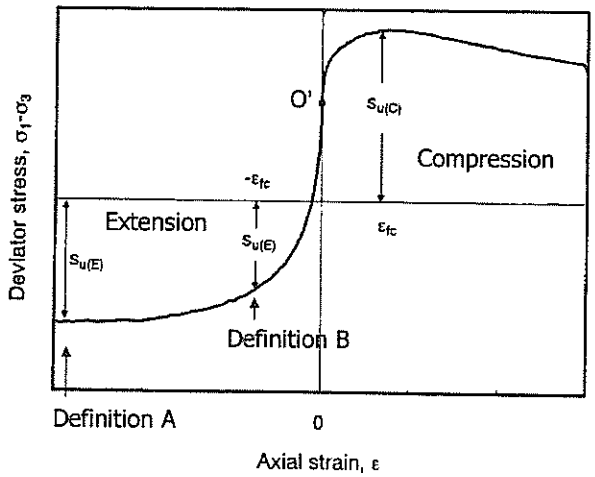

Figure 67 Typical stress-strain curve of Holocene clay

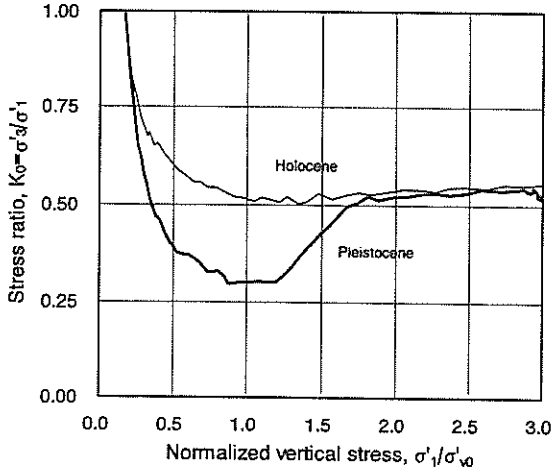

Figure 68 Measured K_0 value with axial consolidation Pressure

Kishida, 1982), the undrained shear strength is defined as the average of compression strength and the extension strength. The problem is how to determine the extension strength. One definition of the extension strength is the maximum strength within the 15 % axial strain.

A typical stress-strain relationship for Japanese Holocene clay observed in CAUC and CAUE is shown in **Figure 67**. The peak strength appeared at a small strain in compression side, while the peak strength in extension side is usually mobilized with the larger strain or sometimes no peak strength is shown within the maximum axial strain of 15%. When extension strength is defined as the maximum strength within the 15% axial strain, the axial strain at the peak strength is much larger than that of compression strength. In addition, extension shear strength is also defined as the strength at the strain when the peak strength is mobilized in compression test. The reason for the latter definition is that the average strength resulted from the compression and extension tests should be considered at the same strain level. The extension strengths obtained by the two definitions were used for design shear strength, and the influences on stability analysis were discussed.

5.4 Test result and discussions

Figure 68 shows the observed variations of K_0-value (= σ'_3/σ'_1) with consolidation stress σ'_1 normalized with the effective overburden stress σ'_{v0} for an Holocene clay obtained from a depth of 21m and a Pleistocene clay from a depth of 53m below the seabed. For the Holocene clay, the K_0-value decreases during over-consolidation range, after that K_0-value reaches a plateau at 0.5 after σ'_{v0}. On the other hand, for the Pleistocene clay, which is relatively an old deposit, the K_0-value decreases remarkably during over-consolidation range to the bottom level around σ'_{v0}. After that K_0 increases, it finally settles in a constant value of 0.5, that is almost the same as that for the Holocene clay. The difference between the alluvial clay and the Pleistocene clay is probably due to the well-developed structures in the Pleistocene clay. In this study, the K_0 value of 0.5 observed for normally consolidation stage is adopted to recover the in situ stresses by anisotropic consolidation for CAUC and CAUE tests.

Figure 69 (a) shows the stress-strain relationships of Pleistocene clay sample of 55 m depth, in which one specimen was consolidated one dimensionally up to the normally consolidated stage of $3\sigma'_{v0}$ and for the other one, the recompression specimen was reconsolidated by σ'_{v0} with K_0=0.5. **Figure 69(b)** shows the effective stress paths of the tests. In compression loading, the normally consolidated clay yielded just at the beginning of shear, shifting from the elastic stage to the plastic stage with

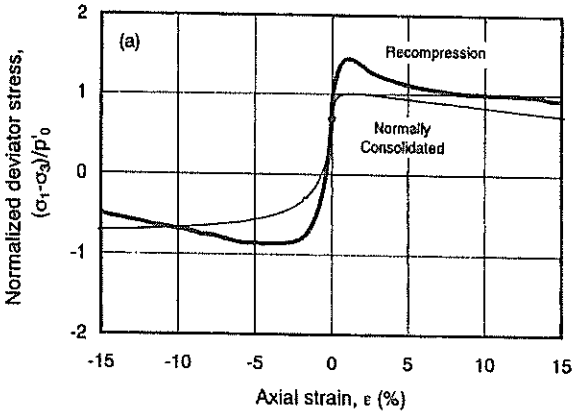

Figure 69(a) Stress-strain curves

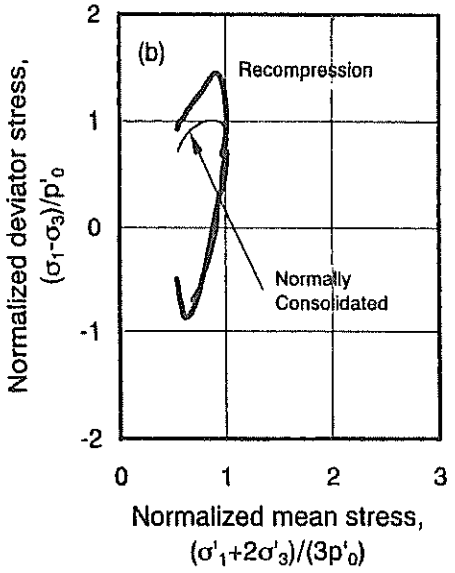

Figure 69(b) Effective stress path

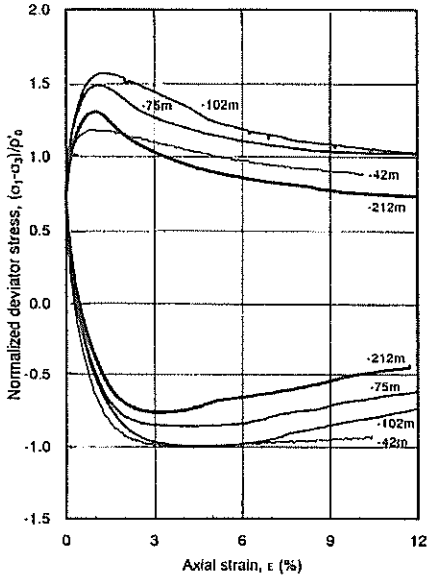

Figure 70 Stress-strain curves of Pleistocene clays of different depths

strain softening behavior. On the other hand, the recompression specimen showed larger yield stress with larger secant modulus, while in the post-yielding region, stress-strain relation and stress path of the recompression specimen were gradually approaching those of the normally consolidated clay. In extension loading, the normally consolidated clay did not have a maximum deviator stress, and the strain hardening behavior were shown even though the axial strain was as much as 15%. However, the specimen of recompression had peak strength with a strain of 2 to 5 % and the strain softening behavior was shown after the yielding.

Figure 70 shows the stress-strain curves of Pleistocene clays of different depths. As indicated in the figure, the samples from the larger depth seem to show more brittle behaviors especially in extension loading. The differences of shear behaviors are related to the modes of failure. The aged Pleistocene clay failed with a clearly defined slip surface for compression and with necking for extension, while, the normally consolidated clay collapses uniformly without local failure. Therefore, it is able to say that characteristics of shearing behavior for a clay changes from ductile to brittle by developing structure due to aging effects.

Profiles of shear strength; s_u, determined by CAUC and CAUE tests with depth are shown in **Figure 71(a)** and **Figure 71(b).** The extension shear strengths were determined by the maximum strength within the 15% axial strain (definition A, **Figure 71(a)**), and the strength at the axial strain when compression strength showed the peak (definition B, **Figure 71(b)**), respectively. In the figure, the shear strengths of the Modified Bjerrum's method $s_{u(M.B.)}$ is defined by the mean of the compression strength $s_{u(C)}$ and the extension strength $s_{u(E)}$, and the $s_{u(SCU)}$ is a strength determined by the simplified CU test with correction factor of 0.75. The strength increases with depth linearly, and this means that, although the geological evidences of the periodical sea level changes are observed, the ground has not experienced major tectonic movements after the deposit.

The strength anisotropy, expressed as the ratio of extension strength to compression strength of Pleistocene clays are plotted in **Figure 72(a).** As shown in the figure, the ratio is about 0.6 when the maximum extension strength is used, while the ratio is about 0.4 when extension strength is at the strain equivalent to the peak compression strength, respectively. Tsuchida and Tanaka (1995) showed that the strength ratio of the typical Holocene marine clays, in which the definition A was used, ranged from 0.6 to 0.8. It can be said that the strength anisotropy of Osaka Bay Pleistocene Clay is large, compared with other marine clays in Japan.

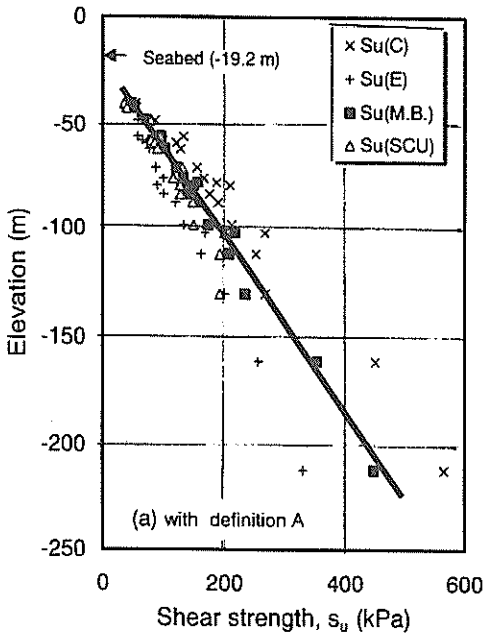

Figure 71(a) Shear strength with depth (extension strength with definition A)

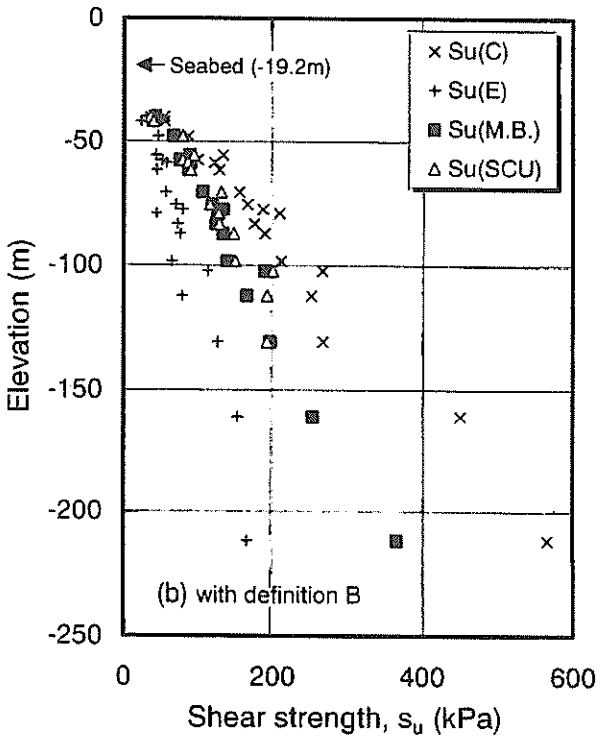

Figure 71(b) Shear strength with depth (extension strength with definition B)

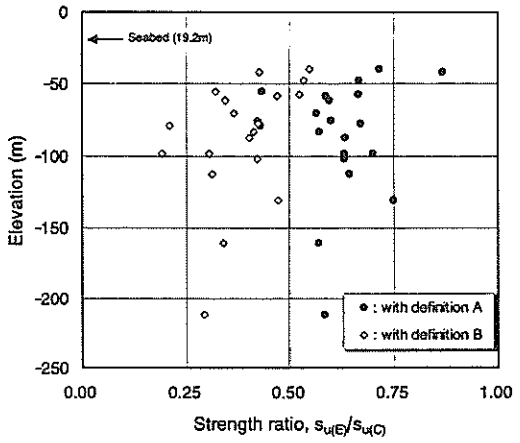

Figure 72(a) Strength anisotropy with plasticity index index

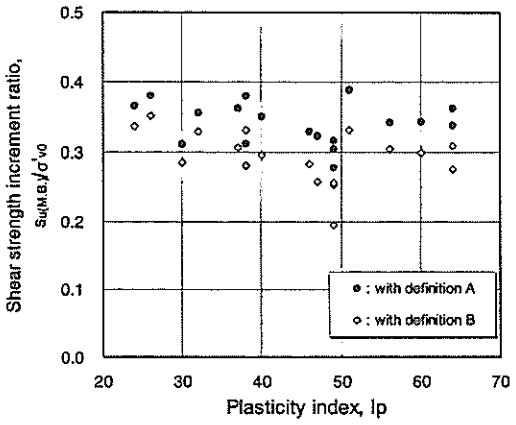

Figure 72(b) Strength increment ratio with plasticity

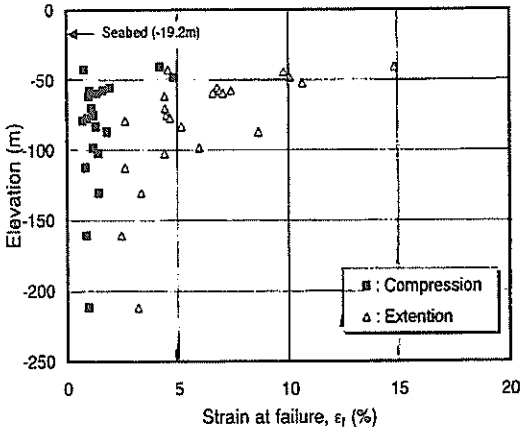

Figure 73 Strain at failure with depth

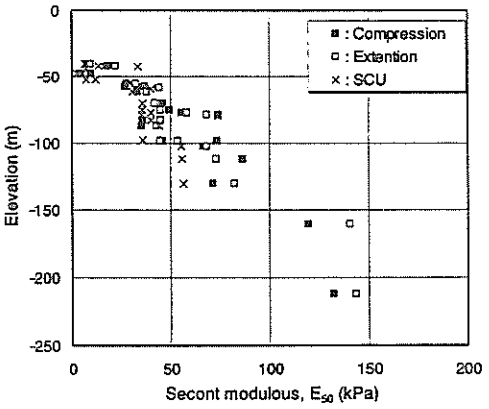

Figure 74 E_{50} with depth

Figure 72(b) shows the relationship between $s_{u(M.B.)}/\sigma'_{v0}$ and the plasticity index I_p. The values of $s_{u(M.B.)}/\sigma'_{v0}$ are 0.3 ~0.5 when the extension strength with definition A is used, and 0.25 ~ 0.40 with definition B. According to the conventional consolidation tests, over-consolidation ratio of Pleistocene clays are between 1.25 and 1.30, therefore by dividing the $s_{u(M.B.)}/\sigma'_{v0}$ with 1.30, strength increment ratio s_u/p in normally consolidation region, is obtained. The s_u/p of the Pleistocene clays were 0.29 when the extension strength with definition A is used, and 0.25 with definition B.

Mesri (1975) pointed out that s_u/p in normally consolidated region of most clay in North America and Europe are 0.22, while Tanaka (1994) showed that the s_u/p of Japanese marine clays ranges from 0.25 to 0.35. The results of Osaka Bay Pleistocene clay confirm the results reported by Tanaka (1994). Taking average value with depth in **Figures 71**, $s_{u(M.B.)}/\sigma'_{v0}$, were 0.34 with the definition A of extension strength, and 0.29 with the definition B. The average normalized strength of the simplified CU test was 0.31.

Figure 73 shows the profiles of strain at failure for the recompression specimens (CAU tests). Strains at failure of compression tests; ε_{fC}, ranges from 2 % to 6% for the Holocene clays, while in Pleistocene clays, most of them are as small as 1%. Strains at failure of extension tests; ε_{fE}, are more than 15% in Holocene clays; while in Pleistocene clays, ε_{fE} were decreased with depth and ranged from 3 to 4% for the depths lower than 80m.

Figure 74 shows the secant modulus, E_{50}, obtained by CAU tests and the **sea** simplified CU test. As shown in the figure, the modulus determined from CAUC and CAUE tests were almost the same, implying that the secant modulus of Pleistocene clay is isotropic. The values of E_{50} obtained from the simplified CU test were smaller by 10-20% than those obtained from CAU tests suggesting that the simplified CU may underestimate E_{50}, because of the difference of consolidation condition.

5.5 Effect of Shear Strength on the stability of -wall structure

Thestability analysis was carried out for the typical seawall structure of Kansai International Airport in the second phase of construction. The assumed cross section is shown in **Figure 75**. The safety factor for the base slide was calculated by the slip circle analysis with modified Fellenius method. **Table 4** shows the assumed material properties used in the stability analyses.

The layer number 11 represents the Pleistocene clay stratum in which the undrained shear strength increasing with the depth is varied corresponding to the triaxial test results. As shown in **Figures 72(a)** and **(b)**, the strength increase ratio; s_u/σ'_{v0} is 0.34 for the average of compression and the maximum extension strengths (definition A), 0.29 for the average strength based on definition B of extension strength, and 0.31 for the Simplified CU test with the correction factor 0.75. Considering these test results, for the range of strength increase ratio, s_u/σ'_{v0} = 0.22 - 0.36, the slip circle analysis was carried out to understand the effect of strength on the safety factor.

Figure 76 shows the calculated variations of the safety factor; F_S, and the bottom depth of slip circle with strength increase ratio; s_u/σ'_{v0}. As shown in the figure, F_S reached a constant value at about 1.29, where s_u/σ'_{v0} is larger than

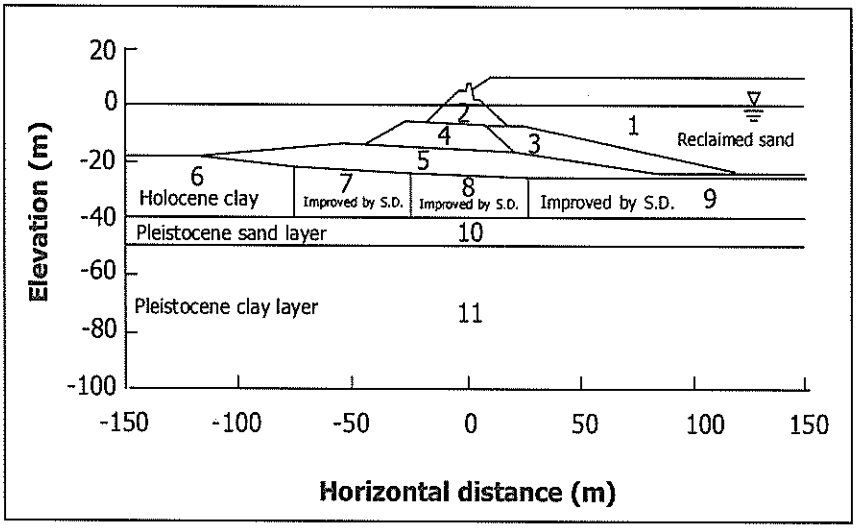

Figure 75 Typical cross section of seawall structure in KIA construction project

Table 4. Parameters for stability analysis

Layers	Soil type	Unit weight (kN/m^3)	Strength parameters
1	Reclaimed sand	19.6	ϕ =30°
2	Concrete caisson	21.6	ϕ =30°
3	Sand	19.6	ϕ =30°
4	Sand	19.6	ϕ =30°
5	Sand	19.6	ϕ =30°
6	Holocene clay, not improved	16.9	s_u = 1.5z (kN/m^2)
7	Holocene clay improved by sand drain	16.9	s_u = 49+ 1.5z (kN/m^2)
8,9	Holocene clay improved by sand drain	16.9	s_u = 118 (kN/m^2)
10	Pleistocene sand	19.6	ϕ = 35°
11	Pleistocene clay	16.9	strength by recompression

z: Initial bottom of sea (DL –19m)

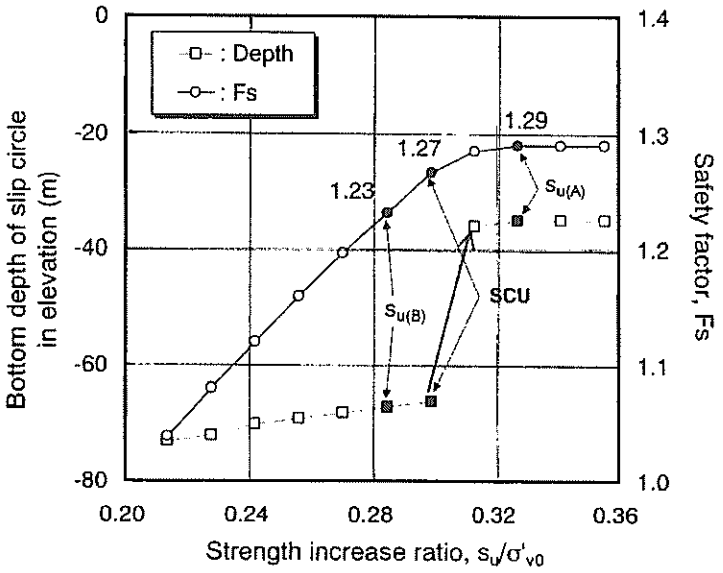

Figure 76 Safety factor and strength of Pleistocene clay

0.32.This is because the critical slip circle is within the Holocene clay layer and did not pass through the Pleistocene deposit layer. When s_u/σ'_{v0} is less than 0.32, F_S is smaller than 1.27, where F_S is increasing linearly with s_u/σ'_{v0}, because the critical slip circle reached the Pleistocene clay deposit and the strength of the Pleistocene clay determined the stability.

Because the shear strength of the sand layer between the Holocene clay layer and Pleistocene clay layer was larger than the strengths of both clay layers the depth of bottom of critical slip circle varied discontinuously at s_u/σ'_{v0} of 0.32.

Figure 77 shows the critical slip circles giving the minimum safety factor in the stability analysis. The $s_{u(peak)}$ corresponds to the average strength with the extension strength of definition A, and the critical circle passes in the Holocene clay. The $s_{u(strain)}$ corresponds to the average strength with the extension strength of definition B, in which the extension strength equivalent to the same strain

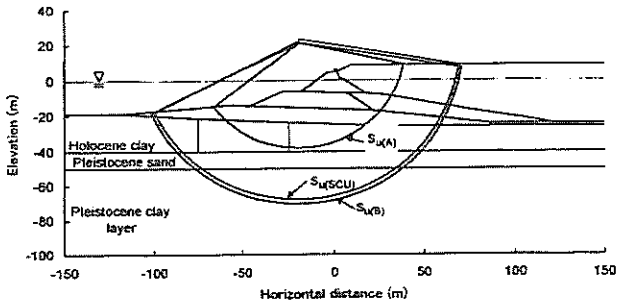

Figure 77 Critical slip circle with different strengths

level as compression, and $s_{u(SCU)}$ corresponds to the strength determined from the simplified CU test. In these 2 cases, the critical slip circles pass through the Pleistocene clay.

As discussed above, depending on the definition of design shear strength, the critical slip circle passes in the Holocene clay layer or in the Pleistocene clay. The results of the stability analysis have shown that, for all the cases of different strength definitions, the minimum safety factor of the seawall structure is larger than 1.20, however the margin for the safety is not so much. The cross section used for stability analysis in **Figure 74** is only an example of the seawall whose length is as much as 10km. When the slip circle passing though the Pleistocene clay layer at great depth may take place, the influenced area of the failure will be quite large and possibly give the serious damage to the whole construction project. Consequently, it is concluded that the accurate estimation of shear strength and the careful stability analysis covering all the construction sites is necessary. Further, the field observations and strict the construction control will be definitely important during the reclamation.

5.6 Summary

The undrained shear strengths and deformation characteristics of Pleistocene clay in Osaka Bay were studied by recompression method with triaxial tests. The conclusions derived from this study are as follows;

1) The shear strength of Pleistocene clay increase linearly with depth, implying that a particular stress history has not been involved.

2) Residual effective stresses in Pleistocene clays collected from large depth were about one fifth of effective overburden stresses. The quality of undisturbed samples of Pleistocene clay are better than the anticipated, although they were collected from large depth.
3) Pleistocene clay at large depths showed brittle stress-strain behavior and it shifts very rapidly from elastic deformation to failure. The clays taken from the depth lower than 80m has peak extension strength at axial strains of 3 ~ 4 %.
4) When the undrained shear strength for design is defined as the average of compression and extension strengths, the strength increase ratio; s_u/σ'_{v0}, depends on the definition of the extension strength. The value of s_u/σ'_{v0} is 0.34 if the extension strength is defined as a peak strength, while the value of s_u/σ'_{v0} was 0.28 if extension strength is defined as strength at the same strain as the compression peak strength, and the value of s_u/σ'_{v0} determined by the simplified CU test was 0.31.
5) The critical slip circle in stability analysis passed thorough the Pleistocene clay layer of the depth of 70m, when the extension strength was defined as strength at the same strain as the compression peak strength. Although the safety factors obtained were larger than 1.20, the margin of the safety were not so much. The accurate estimation of the shear strength of Pleistocene clays and the field observations and construction control will be necessary to complete the projects safely.

6 Conclusions

In recent years, as the scale of structures has been enlarged and the construction works have been carried out in deeper sea areas, the loads due to constructions has become close or larger than the consolidation yield stress, p_c, of the Pleistocene clay layer beneath the Holocene layers. In this report, the compression and shear characteristics of aged Pleistocene clay in Osaka Bay, were reviewed with related to the case study on Kansai International Airport project.

The main conclusions are summarized as follows:

1) The strength gain with time can be divided into 2 components, one of which is associated with volumetric compression, while the other is attributed to the cementation effect. The compression index ratio, r_c is proposed as an index of cementation effect. The value of r_c of Holocene clays and Pleistocene clays in Japan are 1.1-3.0 and 1.1-6.0, respectively, increasing with depth, while r_c of reconstituted young clays are almost 1.0.
2) The high temperature consolidation method was proposed for reproducing the structure of aged clay in laboratory, by consolidating remolded clay slurry under 75° C. This is a useful technique to duplicate aged clay in laboratory.
3) Tan and Tsuchida (1999) investigated the shear strength gain by cementation effect experimentally, and showed that the strength gain by cementation is proportional to elapsed time, and the increment is related to the overburden stress. The strength increment Δs_u can be expressed by the following simple equation;

$$\Delta s_u = 0.3\sqrt{p}\,\Delta(\log t)$$

where, p is an overburden pressure (unit: kN/m^2), and t is an elapsed time after end of primary consolidation. Equation means that the contribution of cementation dominates strength gain with time when the overburden pressure is smaller than 100 kN/m^2, while strength gain due to secondary compression becomes the main component when the overburden pressure is larger than 100 kN/m^2.
4) The concept of standard compression curve (e-log p curve) of clays was proposed. The standard compression curve consists of ultimate standard compression curve, USC, and the standard compression curves from an initial void ratio, SCC(e_0). USC is the e- log p relationship, where e- log p curves converge ultimately with increase of consolidation pressure. SCC(e_0) is the e-log p relationship that starts the consolidation at an initial void ratio e_0. Both curves are determined mainly by the liquid limit of clay and the void ratio at the beginning of consolidation. Using the specific volume index, I_{sv}, which is defined as ln (1+e) / ln (1+e_L), USC and SCC(e_0) were shown as a unique I_{sv} – log p relationship not dependent on the plasticity of clays.
5) Considering the initial condition of marine sediments, the standard relationship between I_{sv} and the effective overburden pressure, σ'_{v0}, was calculated for normally consolidated marine deposits, which is called SCC-marine. By comparing in-situ specific volume of clay with value on of SCC-marine, the degree of structure of marine deposits can be evaluated. It is shown the void ratios of Holocene seabed in the shallow depth can be explained mainly by SCC-marine with no significant effect by aging on the void ratio, and that Osaka Bay Pleistocene clay seems to have well-developed structure due to aging, because the in-situ values of I_{sv} are much larger than those of SCC-marine.
6) Using separated-type consolidometer of high capacity designed in this study, the consolidation characteristics of Osaka Pleistocene clay was examined with the pur-

pose of investigating soil structural effect. Through the tests as a fundamental stage, undisturbed soil in the over-consolidated range showed extremely faster expulsion of excess pore water pressure than the normally consolidated range and that the most part of consolidation settlement is occupied by secondary compression at a given pressure increment.

7) At the pressure increment spanning the consolidation yield stress of Osaka Pleistocene clay, effective stress increasing with elapsed time showed sudden decreasing tendency after the effective stress exceeded the consolidation yield stress. It is estimated that the cause of this unique behavior is to be attributed to the fact that radical increase of compressibility by the yielding of soil structure surpasses the dissipation rate of excess pore water pressure. This behavior is particularly relevant to clays with a well-developed structure such as Osaka Pleistocene clay.
8) The undrained shear strengths and deformation characteristics of Pleistocene clay in Osaka Bay were studied by the recompression method with triaxial tests. Residual effective stresses in Pleistocene clays collected from large depth were about one fifth of effective overburden stresses. Accordingly, the quality of undisturbed samples of Osaka Bay Pleistocene clay was better than anticipated.
9) The Pleistocene clay at large depths is brittle and shifts very rapidly from elastic deformation to plastic failure. The clay obtained from the depth lower than 80m has the peak extension strength at the axial strains of 3 - 4 %.
10) Although the safety factor of slip circle which passes through the Pleistocene clay layer was larger than 1.20, the margin of the safety were not so much. The accurate estimation of the shear strength of Pleistocene clays and the field observations and construction control will be necessary to complete the projects safely.

(Received on February 15, 2002)

Acknowledgements

The study of mechanical properties of Osaka Bay Pleistocene clay has been carried out in Soil Mechanics Laboratory of Port and Airport Research Institute for about 20 years. A number of colleagues in the laboratory have contributed to this study and their assistance is gratefully acknowledged. The authors would like to express special thanks to Mr. Mizuno, K., Ms. Nishida and Mr. Hikiyashiki, H. in preparing the manuscripts.

References

Abdrabbo, M.(1990):"Correlation between index tests and compressibility of Egyptian Clays", *Soils and Foundations*, Vol.30, No.2, pp.128-132.

Aboshi, H, Matsuda, M. and Okuda, M. (1981): "Preconsolidation by separate type consolidometer", Proc. of 10th ICSMFE, Vol.3. pp.572~579.

Arai, Y.(1991):"Construction of an artificial offshore island for the Kansai International Airport", Proceedings of International Conference on Geotechnical Engineering for Coastal Development, Geo-Coast'91,Port and Research Institute. Vol.2, pp.927-943.

Arai, Y., Oikawa, K. and Yamagata, N. (1991):"Large scale sand drain works for the Kansai International Airport", Proceedings of International Conference on Geotechnical Engineering for Coastal Development, Geo-Coast'91, Port and Research Institute. Vol.1, pp.281-286.

Burland, J., B. (1990):"On the Compressibility and Shear strength of Natural Clays", *Geotechnique*, Vol.40, No.3, pp.329-387.

Butterfield, R.(1979):"A natural compression law for soils (an advance on e-log p)",*Geotechnique*, Vol.29, No.4, pp.469-480.

Berre, T. and Iversen, K.(1972): "Oedometer tests with different specimen heights on a clay exhibiting large secondary compression", *Geotechnique* 22. No.1. pp.53-70.

Berre, T. and Bjerrum, L. (1973): "Shear strength of normally consolidated clays", Proc. of the 8th ICSMFE, pp.39-49.

Endo, H., Oikawa, K., Komatsu, A. and Kobayashi, M. (1991):"Settlement of diluvial clay layers caused by a large scale man-made island", Proceedings of International Conference on Geotechnical Engineering for Coastal Development, Geo-Coast'91,Port and Research Institute. Vol.1, pp.177-182.

Gomyo, M., Yauchi, E., Sakai, K., Ohtsuki, T. and Itosu (1985): "On the effect of the mud properties on the interaction between wave and the mud", 33rd Meeting of Coastal Engineering, JSCE, pp.322-326 (in Japanese).

Hanzawa, H. (1982): "Undrained strength characteristics of alluvial marine clays and their application to short term stability problems." Thesis of Dr. Eng., University of Tokyo.

Hanzawa, H. and Kishida, T. (1982): "Determination of in-situ undrained strength of soft clay deposits", Soils and Foundations, vol.22, No.2, pp.1-14.

Horie, H., Zen, K., Ishii, I. and Matsumoto, K. (1984): "Engineering properties of marine clay in Osaka bay, (Part-1) Boring and sampling", *Technical Note of The Port and Harbour Research Institute*, No.498, pp.5-45. (in Japanese)

Hong, Z. and Tsuchida, T.: "On compression characteris-

tics of Ariake clays", *Canadian Geotechnical Journal*, No.36, pp.807-814, 1999.

Imai, G. and Tang, Y. X.(1992): "A constitutive equation of one-dimensional consolidation derived from interconnected tests", *Soil and Foundations*, JSSMFE. Vol. 32. No. 2. pp.83-96.

Imai, G. (1978): "Fundamental Studies on one-dimensional consolidation characteristics of fluid mud", Thesis of Dr. Eng. University of Tokyo.

Ishii, I., Ogawa, F. and Zen, K. (1984) : "Engineering properties of marine clays in Osaka bay, (Part-2) Physical Properties, consolidation characteristics and Permeability", *Technical Note of the Port and Harbour Research Institute*, No.498, pp.47-86. (in Japanese)

Inoue, T., Tan, T. S. and Lee S.L. (1990):"An investigation of shear strength of slurry clay", *Soils and Foundations*, Vol.30, No.4, pp.1-10.

Jamiolkowski, M., Ladd, C.C., Germaine, T.T. and Lancellota, R. (1985): "New developments in field and laboratory testing of soils", State of the Art Report, Proc. of the 11th ICSMFE, pp.57-153.

Japanese Society on Soil Mechanics and Foundation Engineering (1966): Investigation, design and construction in soft ground, Soil Engineering Library 1, pp.92-94. (in Japanese)

Japanese Society on Soil Mechanics and Foundation Engineering (1992): "Fall cone method, Report of Research Committee Ⅲ ", Proceedings of symposium on new method of physical soil testing", pp.69-90. (in Japanese)

Japanese Geotechnical Society (1995): "Method for obtaining undisturbed soil sample using thin-walled tube sampler with fixed piston." JGS 1221-1995.

Kanda, K., Suzuki, S., and Yamagata, N. (1991): "Offshore soil investigation at the Kansai International Airport.", Proc. of GEO-COAST '91, Vol.1, pp.33-38.

Kang, M.-S. and Tsuchida, T. (2000): Experimental study on the consolidation properties of Osaka Pleistocene clay by separated-type consolidometer test, IS-32-44Yokohama2000, 2000.9.(submitted)

Kawakami, H., Abe, H. and Iwasaki, K. (1978): "Influence of suction on unconfined compression strength." Proc. of 13th annual meeting of JSSMFE, pp.313-316. (in Japanese)

Kitazume, M. and Terashi, M. (1994):"Effect of stress-strain characteristics on slope failure", Proceedings of international conference on centrifuge test", Centrifuge 94, Balkema, pp. 611-616.

Kobayashi, M. (1994):"Geotechnical engineering aspects of Kansai International Airport Project", Proceedings of 39th Geo-engineering Symposium, JSSMFE, pp.1-6. (in Japanese)

Ladd, C.C. and Lambe, W. (1963): "The strength of undisturbed clay determined from undrained tests", *ASTM*, STP-361, Laboratory Shear Testing of Soils, pp.342-371.

Ladd, C. C. and Foott, R. (1974): "New Design Procedure for Stability of Soft Clay", Proc. ASCE, GT7, pp.763-786.

Locat, J. and Lefebvre, G. (1985): "The Compressibility and Sensitivity of an Artificially sedimented Clay Soil: The Grande-Baleine Marine Clay, Quebec, Canada", *Marine Geotechnology*, Vol.6, No.1.

Mesri, G. and Choi, Y. K. (1985): " The uniqueness of the end-of-primary (EOP) void ratio-effective stress relationship", Proc. of the 11th ICSMFE, Vol. 2, pp587-590.

Mesri, G. and Godlewski, P. M.(1977): "Time- and stress-compressibility inter-relationship", *Journal of the Geotechnical Engineering Division*. ASCE. Vol.103. No.5. pp.417-430.

Mesri,G.: "New design procedure for stability of soft clays", Discussion, ASCE, GT4, Vol.101, pp.409-412, 1975.

Mikasa, M.(1988):"Liquid limit test by cyclic consolidation", *23rd Annual Conference of J.S.M.F.E.*,pp.267-268. (in Japanese)

Mitachi, T. and Fujiwara, Y. (1987): "Undrained Shear Behavior of Clays Undergoing Long-term Anisotropic Consolidation", *Soils and Foundation*, Vol.27, No.4, pp.45-61.

Mitachi, T. and Kudoh, Y. (1996): "Method for predicting in-situ undrained strength of clays based on the suction value and unconfined compressive strength.", *Journal of Geotechnical Engineering, JSCE*, No.541 / III-35, pp.147-157. (in Japanese)

Nakashima, Y., Kozawa, K., Kiyama, M. and Maegawa, H. (1995): Back analysis of settlement in Osaka Port undersea tunnel, Proc. Of International symposium on compression and consolidation of clayey soils, IS-Hiroshima 95', Vol.1, pp.725-732.

Ogawa, F. and Matsumoto, K. (1978): Correlations of geotechnical parameters in port and harbor area, *Report of the Port and Harbour Research Institute*, Vol.17, No.3, pp.7-20. (in Japanese)

Okumura, T.(1974): "Studies on the disturbance of clay soils and the improvement of their sampling techniques", *Technical Note of Port and Harbour Research Institute*. No. 193. (in Japanese).

Shimizu, M. and Tabuchi, T. (1993): "Effective stress behavior of clays in unconfined compression tests", *Soils and Foundations*, Vol.33, No.3, pp.28-39.

Shogaki, T., Kaneko, M., Moro, H. and Mihara. M. (1995): "Method for predicting in-situ undrained strength of clays by unconfined compression test with suction measurements.", Proc. of Sampling Symposium, JSSMFE. (in Japanese)

Shogaki, T. and Kaneko, M.: "Effects of sample disturbance on strength and consolidation parameters of soft clay", *Soils and Foundations*, Vol.34, No.3, pp.1-10,1994.

Skempton, A.W.(1944) : "Note on the Compressibility of Clays", *Q. J. Geological Society*. Vol.100, pp.119-135.

Skempton A. W.(1970): "The Consolidation of Clays by Gravitational Compaction", *Quarterly Journal of Geological Society of London*, Vol.125, pp.373-412, 1970.

Tan, Y.X. and Tsuchida, T.: The development of shear strength for sedimentary soft clay with respect to aging effect, *Soils and Foundations*, Vol.39, No.6, pp.13-24, 1999.

Tanaka,H. and Tanaka,M.(1994) : Determination of Strength of Clay by means of Vane Shear Test, *Report of the Port and Harbour Research Institute*, Vol.33, No.4, pp.1-17. (in Japanese)

Tanaka, H., Tanaka, M. and Hamouche, K.K.(1997a): "Applicability of unconfined compression test to overseas countries' clays." Proc. of 41th Symposium on Geotechnical Engineering, pp.61-66. (in Japanese)

Tanaka, H. and Tanaka, M. (1997b): "Applicability of unconfined compression test to European clays", Proc. of the 14th ICSMFE, pp.209-212.

Tanaka, H. and Locat, J. (1999): "A microstructural investigation of Osaka Bay clay: the impact of microfossils on its mechanical behavior." *Canadian Geotechnical Journal*, Vol.36, pp.493-508.

Tanaka, M., Tanaka, H., Mitsukuri, K. and Suzuki, K. (1995): "Relation of unconfined compression strength and suction on undisturbed clay samples." , *Proc. of 30th annual meeting of JGS*, pp.621-622. (in Japanese)

Tavenas, F. and Leroueil, S. (1977): "Effects of stresses and time on yielding of clays", Proc. of the 9th ISFMFE, Vol.1, pp.319-326.

Terzhagi, K. and Peck, R. B. (1967): Soil Mechanics in Engineering Practice, 2nd ed. John Wiely and Sons, New York.

Tsuchida, T. (1990): "Study on determination of undrained strength of clayey ground by mean of triaxial tests." *Technical Note of The Port and Harbour Research Institute*, Ministry of Transport, Japan, No.688. (in Japanese)

Tsuchida, T.(1991) :"A New Concept of e-log p Relationship for Clays", Proc. of 9th ARCSMFE., Bangkok, Vol.1, pp.87-90.

Tsuchida, T. (1994):"A unified concept of e-log p relationship", Proc. of 13th Conference of ISSMFE, New Delhi, Vol.1, pp.71-74.

Tsuchida, T. (1995): "Unified model of e-log p relationship with the consideration of the effect on initial void ratio", Proc. of International Symposium on Compression and Consolidation of Clayey Soils,Is-Hiroshima'95, Vol.1, pp. 379-384.

Tsuchida, T. (1999):"Unified model of e-log p relationship of clay and the interpretation of natural water content of marine deposits", Characterization of soft marine clays, pp.185-202. Balkema.

Tsuchida, T. (2000): "Evaluation of undrained shear strength of soft clay with consideration of sample quality", *Soils and Foundations*, Vol.40, No.3, pp.29-42.

Tsuchida, T., Kikuchi, Y., Nakashima, K. and Kobayashi, M. (1984): "Engineering properties of marine clays in Osaka bay, (Part 3) Static characteristics of shear.", *Technical Note of the Port and Harbour Research Institute*, No.498, pp.87-114. (in Japanese)

Tsuchida, T., Mizukami, J., Oikawa, K. and Mori, Y. (1989): "New method for determining undrained strength of clayey ground by means of unconfined compression test and triaxial test." *Report of the Port and Harbour Research Institute*, Ministry of Transport, Japan, Vol.28, No.3, pp.81-145. (in Japanese)

Tsuchida, T. and Kikuchi, Y. (1991): "K_0-consolidation of undisturbed clays by means of triaxial cell." *Soils and Foundations*, Vol.31, No.3, pp.127-137.

Tsuchida, T., Kobayashi, M. and Mizukami, J. (1991):"Effect of aging of marine clays and its duplication by high temperature consolidation":*Soils and Foundations*, Vol.31, No.4, pp.133-147.

Tsuchida, T., Hong, Z., Watabe, Y. and Ogawa, F. (1999): "Relationship of undrained shear strength versus normalized water content for remolded clayey soils", 34th Annual conference on geotechnical engineering, JGS, Vol.1, pp. 543-544. (in Japanese)

Torrance J.K. and Otsubo M. (1995) : Ariake Bay Quick Clay: A Comparison with the General Model, Soils and Foundations,Vol.35,No.1,pp11-19.

Umehara Y. and Zen, K. (1982):"Consolidation characteristics of dredged marine bottom sediments with high water content", *Soils and Foundations*, Vol.22, No.2, pp.40-54.

Watabe, Y. (1999): "Mechanical properties of K_0-consolidation and shearing behavior observed in triaxial tests for five worldwide clays –Drammen, Louiseville, Singapore, Kansai and Ariake clay", Characterization of Soft Marine Clays, Balkema.

Watabe, Y., Tsuchida, T. and Adachi, K. (2000a): "Undrained shear strength of Pleistocene clay in Osaka Bay and its effect on the stability of a large scale seawall structure." Proc. of IS-Yokohama (submitted)

Yashima, S. (1986) :Pulverulence and properties of pulverulence, Chemical Engineering Series, No.10, Baihukan, pp.54-100. (in Japanese)